vol. 191, no. 4 the american naturalist april 2018

E-Article

Evolution of Genetic Variance during Adaptive Radiation

Greg M. Walter,[1,*] J. David Aguirre,[1,2] Mark W. Blows,[1] and Daniel Ortiz-Barrientos[1]

1. University of Queensland, School of Biological Sciences, St. Lucia, Queensland 4072, Australia; 2. Massey University, Institute of Natural and Mathematical Sciences, Auckland 0745, New Zealand

Submitted January 26, 2017; Accepted September 13, 2017; Electronically published January 31, 2018

Online enhancements: supplemental material. *Dryad data:* http://dx.doi.org/10.5061/dryad.m248h.

abstract: Genetic correlations between traits can concentrate genetic variance into fewer phenotypic dimensions that can bias evolutionary trajectories along the axis of greatest genetic variance and away from optimal phenotypes, constraining the rate of evolution. If genetic correlations limit adaptation, rapid adaptive divergence between multiple contrasting environments may be difficult. However, if natural selection increases the frequency of rare alleles after colonization of new environments, an increase in genetic variance in the direction of selection can accelerate adaptive divergence. Here, we explored adaptive divergence of an Australian native wildflower by examining the alignment between divergence in phenotype mean and divergence in genetic variance among four contrasting ecotypes. We found divergence in mean multivariate phenotype along two major axes represented by different combinations of plant architecture and leaf traits. Ecotypes also showed divergence in the level of genetic variance in individual traits and the multivariate distribution of genetic variance among traits. Divergence in multivariate phenotypic mean aligned with divergence in genetic variance, with much of the divergence in phenotype among ecotypes associated with changes in trait combinations containing substantial levels of genetic variance. Overall, our results suggest that natural selection can alter the distribution of genetic variance underlying phenotypic traits, increasing the amount of genetic variance in the direction of natural selection and potentially facilitating rapid adaptive divergence during an adaptive radiation.

Keywords: adaptive radiation, genetic constraint, additive genetic variance, phenotypic divergence, covariance tensor.

Introduction

Evolutionary biologists have long sought to understand the processes that have created the dramatic diversification of species we see in nature (Arnold et al. 2001). Adaptive radiation is one process that drives the creation of biological diversity and occurs when groups of organisms colonize and rapidly adapt to multiple contrasting environments, leading to divergence and speciation (Schluter 2000). Differences in directional selection between environments can favor adaptive phenotypic divergence between populations and lead to the formation of ecotypes (Abbott and Comes 2007; Lowry 2012), provided there is sufficient genetic variation present in those populations (Blanquart et al. 2012). However, experimental work on understanding how spatial variation in natural selection creates adaptive radiation across multiple contrasting environments is rare (e.g., Schluter 1995; Losos et al. 2001; Alcantara et al. 2010).

Replicate populations that occupy similar environments and possess similar phenotypes can be used as natural experiments to explore how genetic and phenotypic variation has evolved during adaptive divergence. Populations that experience similar environments often evolve similar phenotypes, creating strong correlations between habitat and morphology (Schluter et al. 2004; Foster et al. 2007; Eroukhmanoff et al. 2009). If populations adapted to contrasting environments evolve specific traits and these environments are patchily distributed across the landscape, then we might also expect adaptive divergence to result in the evolution of discontinuous phenotypes across a heterogeneous landscape (Lowry et al. 2014). For example, stickleback fish have exhibited rapid adaptive divergence in morphology into a novel environment via the repeated fixation of alleles from standing genetic variation (Colosimo et al. 2005; Barrett et al. 2008), and *Anolis* lizards have repeatedly evolved specialized limbs in similar habitats on different islands (Losos 1990; Losos et al. 2001; Langerhans et al. 2006).

Correlations between habitat and morphology are often examined on single traits in isolation, but natural selection typically acts on multiple traits simultaneously (Dobzhansky 1956; Lewontin 1970; Cheverud 1982; Lande and Arnold 1983; Walsh and Blows 2009; Blows and McGuigan 2015). Consequently, adaptation can favor the evolution of beneficial combinations of traits within an environment and create adaptive divergence in multivariate phenotypes between contrasting environments (Bégin and Roff 2004; Langerhans and DeWitt 2004; Nosil et al. 2009), potentially underlying

* Corresponding author; e-mail: gregory.walter@uqconnect.edu.au.

ORCIDs: Walter, http://dx.doi.org/0000-0002-0883-3440; Aguirre, http://dx.doi.org0000-0001-7520-441X; Blows, http://dx.doi.org/0000-0002-1065-5524; Ortiz-Barrientos, http://dx.doi.org/0000-0002-7493-416X.

Am. Nat. 2018. Vol. 191, pp. E000–E000.
DOI: 10.1086/696123

the origin of ecotypes during adaptive radiation (Schluter 2000; Kolbe et al. 2011; Lowry 2012). Since populations exposed to similar environments can also diverge as a consequence of random drift, quantifying ecotypic divergence requires comparing the divergence in multivariate phenotypes among ecotypes to differences among replicate populations within an ecotype (Lande 1979; Zeng 1988; Bookstein and Mitteroecker 2014). Stronger morphological divergence between ecotypes from contrasting environments than between populations from the same environment suggests that habitat differences have promoted divergence (Langerhans and DeWitt 2004; McGuigan et al. 2005; Langerhans et al. 2006). Such experimental systems can be used to identify how divergent natural selection has created adaptive phenotypic evolution during an adaptive radiation (Schluter 1996).

The magnitude of additive genetic variance in the direction of selection determines the rate of adaptive phenotypic evolution, but the availability of standing genetic variance in multivariate phenotypes depends on the extent of genetic correlation between traits (Lande 1979, 1980; Cheverud 1984; Zeng 1988; Arnold et al. 2008). Genetic correlations among traits concentrate genetic variation into particular trait combinations at the expense of other trait combinations (Arnold 1992). When genetic correlations bias the distribution of genetic variation away from the direction of selection, constraints on the rate of adaptive evolution are likely (Walsh and Blows 2009). The additive genetic variance-covariance matrix (**G**) summarizes the genetic relationships between traits, providing the framework to investigate multivariate phenotypic evolution (Lande 1979). Adaptation is expected to be biased in the direction of the multivariate axis of greatest genetic variance ($\boldsymbol{g}_{\max}$; Schluter 1996, 2000; McGuigan et al. 2005; Chenoweth et al. 2010) at least in the early stages of divergence, as there is little reason to expect that $\boldsymbol{g}_{\max}$ will be in a similar direction to that of natural selection following colonization of a novel environment (Zeng 1988; Schluter 1996).

Divergent selection changes the mean of phenotypes, but it can also change the genetic variance underlying traits. For example, rare alleles held at mutation selection balance may become beneficial when exposed to a new environment, rapidly altering the phenotype mean as well as the distribution of genetic variance (Turelli 1984; Carriere and Roff 1995; Agrawal et al. 2001; Zhang and Hill 2005). Standing genetic variation is readily accessible to natural selection, allowing adaptation to occur rapidly (Barrett and Schluter 2008). If genetic variance can increase in the direction of natural selection such that $\boldsymbol{g}_{\max}$ aligns toward a phenotypic optimum, then adaptation from standing genetic variation may explain how rapid divergence occurs during adaptive radiation (Eroukhmanoff 2009).

In attempting to characterize an adaptive radiation, ideally we would quantify the divergence in multivariate mean (fig. 1*A*) and explore whether genetic variance underlying multivariate phenotypes has also evolved (fig. 1*B*). If we observe a change in both the multivariate mean and underlying genetic variance, we can then ask whether changes in multivariate phenotypic mean align with changes in genetic variance during adaptive radiation (fig. 1*C*, 1*D*). More specifically, we can also ask whether changes in the orientation of genetic variance (divergence in $\boldsymbol{g}_{\max}$) have occurred (fig. 1*E*) and whether such changes also align with divergence in phenotypic mean (fig. 1*F*). Such alignment between divergence in genetic variance and phenotype mean can reveal whether genetic variance can evolve in response to divergent natural selection to facilitate adaptive radiation. Here, we report a set of experiments that enabled us to determine how the phenotypic mean and genetic variance have diverged in the early stages of an adaptive radiation, providing insights into how natural selection shapes the genetic basis of phenotypic evolution.

We investigated the adaptive radiation of the *Senecio lautus* species complex, an herbaceous wildflower native to Australia, New Zealand, and several Pacific Islands. Although *S. lautus* contains many taxonomic species, we focused on varieties within *Senecio pinnatifolius*, which are native to Australia and occupy a diverse array of habitats. We investigated divergence of populations from four distinct habitats: coastal headlands (*S. pinnatifolius* var. *maritimus*; headland ecotype), coastal sand dunes (*S. pinnatifolius* var. *pinnatifolius*; dune ecotype), moist tableland rainforests (*S. pinnatifolius* var. *serratus*; tableland ecotype), and dry sclerophyll woodland (*S. pinnatifolius* var. *dissectifolius*; woodland ecotype; Ali 1969; Radford et al. 2004). Ecotypes from these habitats display strong morphological differentiation associated with the different environments. Plants maintained their field morphology when grown under common garden conditions, indicating that phenotypic differences between populations have a strong underlying genetic basis (Ali 1964, 1969; Ornduff 1964; Radford et al. 2004). Transplant experiments have revealed that these ecotypes are adapted to their local environments (Melo et al. 2014; Richards et al. 2016; Walter et al. 2016), where extrinsic reproductive isolation is strong but intrinsic reproductive isolation is weaker, suggesting that barriers are largely geographic and ecological (Melo et al. 2014; Richards and Ortiz-Barrientos 2016; Richards et al. 2016; Walter et al. 2016). Phylogenetic and population genetic analyses have revealed two young clades of taxa with low genetic differentiation yet high levels of morphological diversity (Roda et al. 2013*a*, 2013*b*). Divergence between clades is less than half a million years, and some ecotypes (coastal and alpine) have formed independently multiple times, suggesting that, similar to other systems (e.g., African cichlids [Muschick et al. 2012] and the Caribbean *Anolis* lizards [Langerhans et al. 2006]), the *S. lautus* species complex has recently undergone parallel

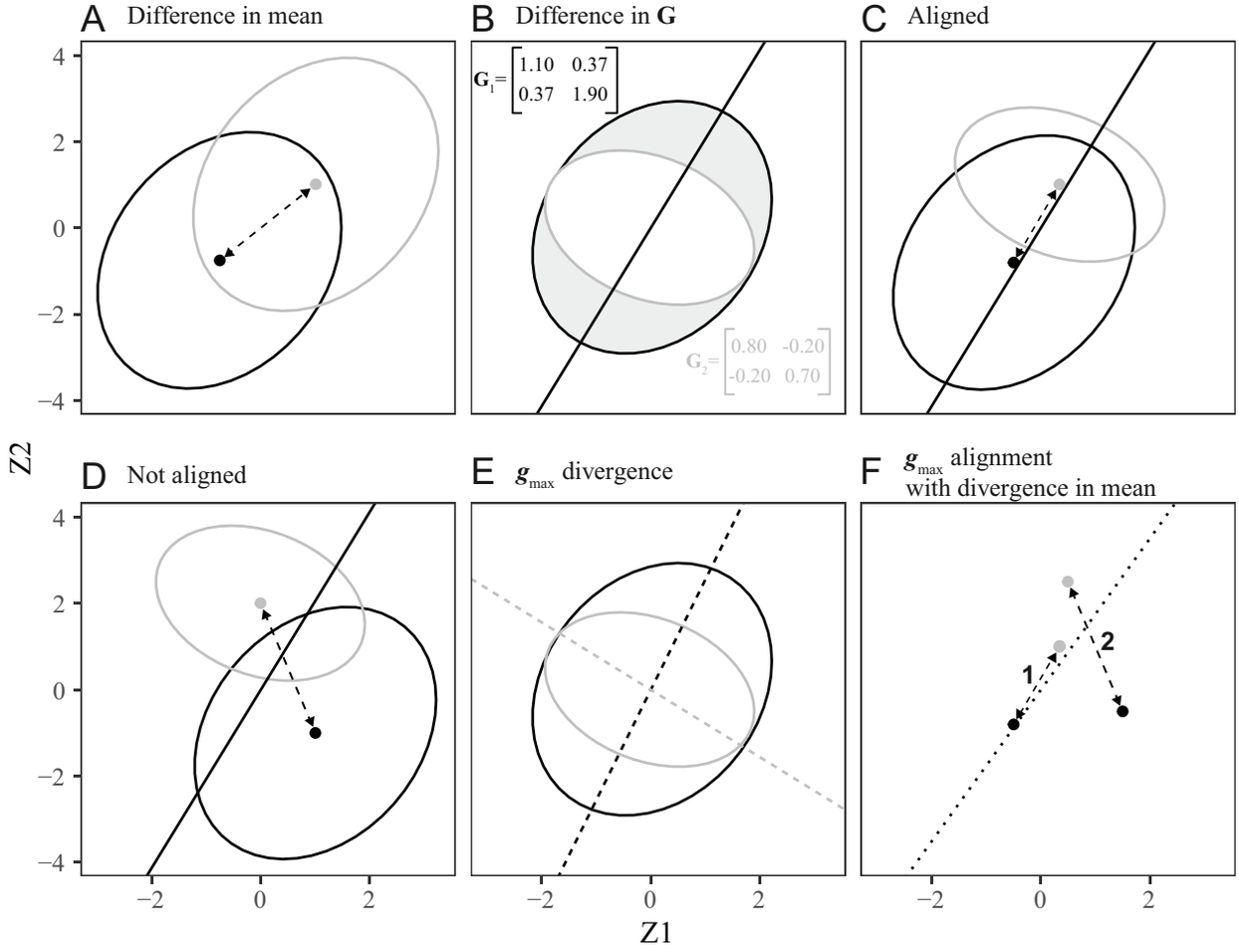

Figure 1: Visualizing multivariate divergence in mean and genetic covariance structure in two dimensions between ecotype 1 (black ellipses and filled circles) and ecotype 2 (gray ellipses and filled circles). For two traits (Z1 and Z2) under six different scenarios, we show the position of ecotype means (filled circles), genetic covariance structure (ellipses), and the direction of change in phenotype means (dotted double arrows) relative to the axis of greatest change in genetic variance (*B–D*; solid line) and change in the orientation of genetic variance (*E*, *F*; dashed lines). *A*, Different mean phenotypes but with the same genetic covariance structure. *B*, Same mean phenotype but divergence in genetic covariance where ecotype 1 ($\mathbf{G}_1$) has a positive genetic covariance while ecotype 2 ($\mathbf{G}_2$) has a negative covariance between traits. Gray shading denotes the difference in genetic variance, while the solid line represents the leading eigenvector of the difference matrix $\Delta\mathbf{G} = \mathbf{G}_1 - \mathbf{G}_2$, which can be generalized to a fourth-order tensor in more complex situations discussed later in the main text. *C*, If genetic variance can evolve to facilitate adaptive radiation, changes in genetic covariance structure will align with changes in mean, and ecotype means will be separated along the axis of divergence in genetic covariance (solid line vs. dashed arrow). *D*, However, if changes in mean phenotype do not align with changes in genetic covariance, multivariate trait means will separate along an axis different to the axis of divergence in genetic covariance. *E*, Genetic changes may also change the orientation of **G**, shown by the differences in $\boldsymbol{g}_{max}$ for each ecotype (gray vs. black dashed lines). *F*, If the orientation of **G** has evolved and divergence in the orientation of $\boldsymbol{g}_{max}$ (captured by the dotted line) aligns with divergence in phenotype mean 1, then **G** has evolved and adaptive divergence has occurred along $\boldsymbol{g}_{max}$ in each habitat. However, if divergence in $\boldsymbol{g}_{max}$ does not align with divergence in mean phenotype 2, then although **G** has evolved, evolution has not occurred along $\boldsymbol{g}_{max}$.

evolution and adaptive radiation (Roda et al. 2013*a*, 2013*b*; Melo-Hurtado 2014).

To investigate how divergence in mean multivariate phenotype has occurred among ecotypes (fig. 1*A*), we sampled seeds from replicate populations of each of the four ecotypes, grew these under common garden conditions, and measured 10 traits related to plant architecture and leaf morphology. In a separate experiment, we used a breeding design to estimate additive genetic (co)variance matrices for each ecotype for the same 10 morphological traits, to quantify divergence in genetic variance among ecotypes (fig. 1*B*). Finally, to investigate how adaptive divergence has

occurred during a radiation, we investigated whether divergence in genetic variance and divergence in phenotypic mean were aligned (fig. 1*C*–1*F*). Here, we propose that genetic variance can evolve in response to strong divergent natural selection, promoting the evolution of beneficial genetic correlations among traits that facilitate rapid adaptive divergence following the colonization of novel contrasting environments.

Methods and Material

Glasshouse Experiments

We collected seeds from four populations of each ecotype (table A1). Populations occupy small patches of habitat, which restricted us to sampling seeds from 30–45 individuals per population. Seeds were taken from individuals at 10-m intervals to reduce the risk of sampling close relatives. To compare divergence in phenotypic mean with divergence in genetic variance, we conducted two separate glasshouse experiments. First, to estimate divergence in multivariate phenotype mean, we grew 16 individuals from four populations of each ecotype (ecotype $n = 4$; population $n = 16$; total $N = 242$) in a common garden. Second, we used a breeding design to estimate genetic variance components for two populations of each ecotype (ecotype $n = 4$; population $n = 8$; total $N = 1{,}259$). Data for both experiments are deposited in the Dryad Digital Repository: http://dx.doi.org/10.5061/dryad.m248h (Walter et al. 2018).

To estimate genetic variance, we grew two generations of plants in the glasshouse. To establish the parent generation, we grew seeds collected from the natural populations. Seeds taken from a single plant in the native populations were likely pollinated by different individuals, making parentage uncertain. Therefore, we grew only one seed from each individual sampled in the field, giving a parental generation of 32–46 individuals per population (table A2). To estimate additive genetic variance, we implemented a crossing design using individuals from the parent generation. Half of the individuals from each population were designated sires ($n = 17$–23 per population; table A2), and the other half were designated dams ($n = 15$–23 per population; table A2). For each population, two randomly selected sires were then mated to two randomly selected dams in all possible combinations. Additive genetic variance was estimated as the variance between paternal half-siblings (Lynch and Walsh 1998). Three or four offspring for each full-sibling family (totaling 934 individuals) produced from these crosses were grown and phenotyped in the glasshouse experiment.

Estimating genetic variance requires large sample sizes even when using established breeding designs (Lynch and Walsh 1998), which logistically restricted us to only two populations for each ecotype. However, measuring divergence in multivariate phenotype mean is best achieved using a hierarchical framework by assessing differences between ecotypes, while taking into account differences between populations within ecotypes (Bookstein and Mitteroecker 2014). As such, we used the first experiment with four populations per ecotype ($df = 3$) to estimate divergence in multivariate phenotype mean. Differences in mean phenotypes between populations grown in both experiments were minor (fig. S1; figs. S1–S5 are available online).

Growth Protocol and Phenotype Measurement

To grow seeds in the glasshouse, we induced seed germination by scarifying each seed with a razor blade, placing them on moist filter paper in glass petri dishes and leaving them in the dark for 2 days. Seedlings were then transferred to a controlled-temperature room at 25°C on a 12L : 12D light cycle. After 1 week, seedlings were taken to the glasshouse and planted into 137-mm round pots in glasshouse experiment 1 and 85-mm square pots in glasshouse experiment 2. Pots contained soil (70% pine bark : 30% coco peat) with 5 kg/m^3 osmocote slow-release fertilizer and 830 g/m^3 Suscon Maxi soil insecticide. We performed controlled crosses between plants by rubbing two mature flower heads together over successive days, allowing each flower to receive and donate pollen. Seeds were collected once mature and stored at 4°C until required for subsequent experiments.

Ten morphological measurements were taken using identical methods in both glasshouse experiments. Architectural measurements were recorded to the nearest millimeter with a ruler and included plant vegetative height, plant width at the widest point, plant width at the narrowest point, and main stem length. Secondary branches were counted, and main stem diameter was measured with callipers 1 inch from ground level. We divided the main stem length by an average of the two width measurements to get an architectural measurement that encompassed plant growth habit. One young but fully expanded leaf was taken from each plant and scanned using a flatbed scanner. Morphometric data of all scanned leaves were extracted using the program Lamina (Bylesjo et al. 2008). Traits produced by Lamina included leaf area, perimeter, circularity, indent (serrations and lobes) width, indent depth, and indent number. Perimeter squared divided by area squared was calculated as a measure of leaf complexity. Indent number was divided by perimeter to calculate indent density along the margin of the leaf.

Phenotypic traits for both experiments were normally distributed, but because traits were measured on different scales, we standardized traits to prevent differences in measurement units from dictating the distribution of phenotypic and genetic variation (Hansen and Houle 2008; Houle et al. 2011). In experiment 1, we standardized globally by standardizing the trait measurements for all individuals of all eco-

types and populations to a mean of 0 and standard deviation of 1. In experiment 2, we standardized locally by standardizing the trait measurements for all individuals within each ecotype to a mean of 0 and standard deviation of 1. Different strategies of standardization were implemented because divergence in multivariate phenotype is relative among ecotypes, whereas we were interested in comparing absolute differences in genetic variance between ecotypes.

Divergence in Multivariate Mean among Ecotypes

To investigate divergence in mean phenotype, we conducted a MANOVA in R (v. 3.3.2) using the nested linear model

$$\mathbf{y}_{ijk} = \boldsymbol{\mu} + \mathbf{E}_i + \mathbf{P}(\mathbf{E})_{j(i)} + \mathbf{e}_{k(ij)}, \quad (1)$$

where $\boldsymbol{\mu}$ was the intercept, and the sources of variation in the experiment were represented by ecotype ($\mathbf{E}_i$), populations nested within ecotype ($\mathbf{P}(\mathbf{E})_{j(i)}$), and the residual error ($\mathbf{e}_{k(ij)}$). The 10 traits were fitted as a multivariate response variable ($\mathbf{y}_{ijk}$). From the MANOVA, we calculated the **D** matrix by extracting the sums of squares and cross-product matrices for ecotype ($\text{SSCP}_\mathbf{E}$) and population ($\text{SSCP}_\mathbf{P}$) to calculate the mean squares matrices for each term by dividing each matrix by their corresponding degrees of freedom ($\text{MS}_\mathbf{E} = \text{SSCP}_\mathbf{E}/3$; $\text{MS}_\mathbf{P} = \text{SSCP}_\mathbf{P}/12$). We then calculated **D** using

$$\mathbf{D} = (\text{MS}_\mathbf{E} - \text{MS}_\mathbf{P})/nf, \quad (2)$$

where *nf* represented the number of individuals sampled from each ecotype in a balanced design. Given slight differences in numbers between ecotypes, we calculated *nf* using equation (9) in Martin et al. (2008). We used this method for calculating **D** to isolate the divergence between ecotypes from differences between populations (Martin et al. 2008). Eigenanalysis of **D** gave the linear combination of traits that described divergence in mean phenotype between ecotypes with the associated eigenvalue representing the amount of divergence. Three degrees of freedom at the ecotype level gave a maximum of three nonzero eigenvectors for **D**. To test the significance of **D**, we created a null expectation for **D** by randomizing individual phenotypes between ecotypes 1,000 times and recalculating **D** for each randomized data set.

Estimation of Multivariate Genetic Variance

To estimate the genetic variance components for each ecotype, we used the R package MCMCglmm (Hadfield 2010) to fit the model

$$\mathbf{y}_{ijkl} = \boldsymbol{\mu} + \mathbf{P}_i + \mathbf{S}_{j(i)} + \mathbf{M}_{k(ij)} + \mathbf{S}_{j(i)} \times \mathbf{M}_{k(ij)} + \mathbf{e}_{l(ijk)}, \quad (3)$$

where replicate population ($\mathbf{P}_i$) and the intercept ($\boldsymbol{\mu}$) were fitted as fixed effects. Modest replication of phenotyped offspring within each population prevented us from confidently estimating genetic variance for each population. Nonetheless, including replicate population as a fixed effect removed the variation due to difference in means between populations (i.e., population divergence) and allowed us to estimate genetic variance for each ecotype. Sire ($\mathbf{S}_{j(i)}$), dam ($\mathbf{M}_{k(ij)}$), and the sire × dam interaction ($\mathbf{S}_{j(i)} \times \mathbf{M}_{k(ij)}$) were fitted as random effects, and $\mathbf{e}_{l(ijk)}$ was the residual variance. Each trait ($\mathbf{y}_{ijkl}$) was standardized to a mean of 0 and standard deviation of 1 (within each ecotype) before being entered as a multivariate response. We implemented each model with 2,100,000 Markov chain Monte Carlo (MCMC) sampling iterations, which included a burn-in of 100,000 MCMC iterations and a thinning interval of 2,000 MCMC iterations. We used a Cauchy prior distribution for the variance components (Gelman 2006), with a location parameter of 0 and a scale parameter of 1. To examine the sensitivity of the prior, we adjusted the parameters to excessively large and small values, making sure the parameter estimates remained stable. All models converged with autocorrelation below 0.05 between MCMC sampling iterations, and the effective sample size exceeded 85% of the total number of samples for all parameters estimated. We then calculated the additive genetic variance matrix, **G** ($\mathbf{G}_{\text{obs}}$) as four times the sire-level covariance matrix ($\mathbf{S}_{j(i)}$; Lynch and Walsh 1998).

Estimates of variance components produced by MCMCglmm are constrained to be greater than 0 (positive-definite), making comparisons of posterior distributions to 0 an uninformative test of significance. To test the significance of the estimated variance components and their subsequent analyses, we produced a suitable null expectation by randomizing the observed data (Aguirre et al. 2014*a*; McGuigan et al. 2015). For each ecotype, we randomized the phenotypes of individuals among families and reimplemented equation (3). Nonzero estimates of variance components derived from models implemented on randomized data provided estimates of the distribution of genetic variance expected by chance, given our data and our model. A difference between the parameter estimates for the randomized and observed data provides evidence that the patterns in the observed data are biological.

The randomization procedure used here differs slightly from previous studies, which created a null distribution by collecting multiple samples from the posterior distributions of multiple models implemented on different randomizations of the data (Aguirre et al. 2014*a*; McGuigan et al. 2015). Posterior samples from the same randomization capture the uncertainty in the parameter estimates for that particular randomization but do not provide independent estimates of the uncertainty introduced by the randomization procedure itself. To create a null distribution that focused

on the uncertainty introduced by the randomization procedure and center our inference on the significance of the observed posterior mean, we used a null distribution ($\mathbf{G}_{null}$) constructed from the posterior means of 1,000 models, each conducted on a single randomization of the data. Our procedure more closely resembles a posterior predictive distribution commonly used to assess how well a model fits the underlying observed data. Accordingly, rather than comparing the overlap between null and observed posterior distributions, our significance test for the posterior mean is based on the overlap of the null distribution of posterior means (calculated from the 1,000 randomizations of the data) with the observed posterior mean.

The consequence of implementing a model for each of the 1,000 randomizations of the data is a linear increase in computational time required. However, the use of batch processing on high-performance computer clusters can significantly reduce the total time required to complete the analysis. Furthermore, although the burn-in and thinning intervals for the models based on the observed and randomized data should remain constant to help avoid differences in the mixing of the MCMC chains, it is possible to reduce the total number of iterations. As we were interested only in estimating the posterior mean for each of the 1,000 models, we used our observed models to find the total number of iterations required to obtain a stable estimate of the posterior mean. For our data, the estimate of the posterior mean remained stable after 150 iterations (fig. S2), so we terminated the MCMC chain for the analysis of each randomized data set after 150 iterations, reducing computational time substantially while obtaining robust estimates of the posterior mean for each randomization.

Characterizing **G**

Traits were standardized to a variance of 1 within each ecotype separately, and therefore the diagonal elements of our observed **G** represented the trait heritabilities. To identify whether our estimated heritabilities were greater than expected by chance, we compared the heritabilities of our posterior mean observed **G** with those taken from our randomized **G** matrices. If the heritability estimates from our observed **G** were greater than the 95% highest posterior density (HPD) interval for the randomized heritability distribution, we took this as evidence that our observed heritabilities were greater than expected by sampling error.

To explore the distribution of genetic variance, we used eigenanalyses on posterior mean observed **G**. The distribution of genetic variance among eigenvectors describes the shape of multivariate genetic variance, where fewer eigenvectors with relatively high genetic variance denote a more elliptical **G**. The linear combination of traits with the most genetic variance then describes the direction of greatest multivariate genetic variance ($\boldsymbol{g}_{max}$). To quantify whether eigenvectors described more variance than expected by sampling error, we used two comparisons. First, we compared eigenanalyses conducted on $\mathbf{G}_{obs}$ with $\mathbf{G}_{null}$, which provided a conservative null expectation for the amount of variance captured by $\boldsymbol{g}_{max}$. To do so, we conducted an eigenanalysis on each of the 1,000 random **G** matrices and saved the eigenvalues, which gave the distribution of eigenvalues for the randomized **G**. Second, we projected the observed eigenvectors of **G** through $\mathbf{G}_{null}$, providing an estimate of the null variance captured along our specific observed linear trait combinations. If the eigenvalues from our observed **G** were greater than the upper 95% confidence interval for the distribution of the two calculations of randomized distributions above, then our observed eigenvectors described more variance than expected due to sampling error.

Divergence in Multivariate Genetic Variance among Ecotypes

The difference between two matrices **A** and **B** can be described using the difference $\mathbf{C} = \mathbf{A} - \mathbf{B}$. Eigenanalysis of **C** finds the eigenvectors that describe the axes along which **A** and **B** differ, as well as the eigenvalues describing the magnitude of the difference captured by each eigenvector (see also fig. 1). The covariance tensor (Basser and Pajevic 2007; Hine et al. 2009) is a generalization of this approach that can be used to describe the differences among more than two matrices (fig. 2). The covariance tensor (Σ) is constructed from the variances and covariances between the elements of the original matrices. The covariance tensor framework is then founded on a hierarchy consisting of eigenvalues (α) and eigentensors (**E**) of the tensor, followed by eigenvalues (λ) and eigenvectors of the eigentensors (for detailed methods, see R code, available online; Hine et al. 2009; Aguirre et al. 2014*b*).[1] In the covariance tensor framework, the **C** matrix is a single eigentensor, and the eigenanalysis of **C** provides the eigenvectors and eigenvalues of the eigentensor.

Eigentensors are constructed in such a way that each eigentensor describes an independent axis of difference among the original genetic variance matrices, with the magnitude of the difference in genetic variance determined by the corresponding eigenvalue of the eigentensor (see Hine et al. 2009; Aguirre et al. 2014*b*). The eigentensor with the largest eigenvalue describes the greatest difference in genetic variance among the original matrices, with the subsequent eigentensors forming an orthogonal series of spaces describing incrementally smaller differences in genetic variance

1. Code that appears in the *American Naturalist* is provided as a convenience to the readers. It has not necessarily been tested as part of the peer review.

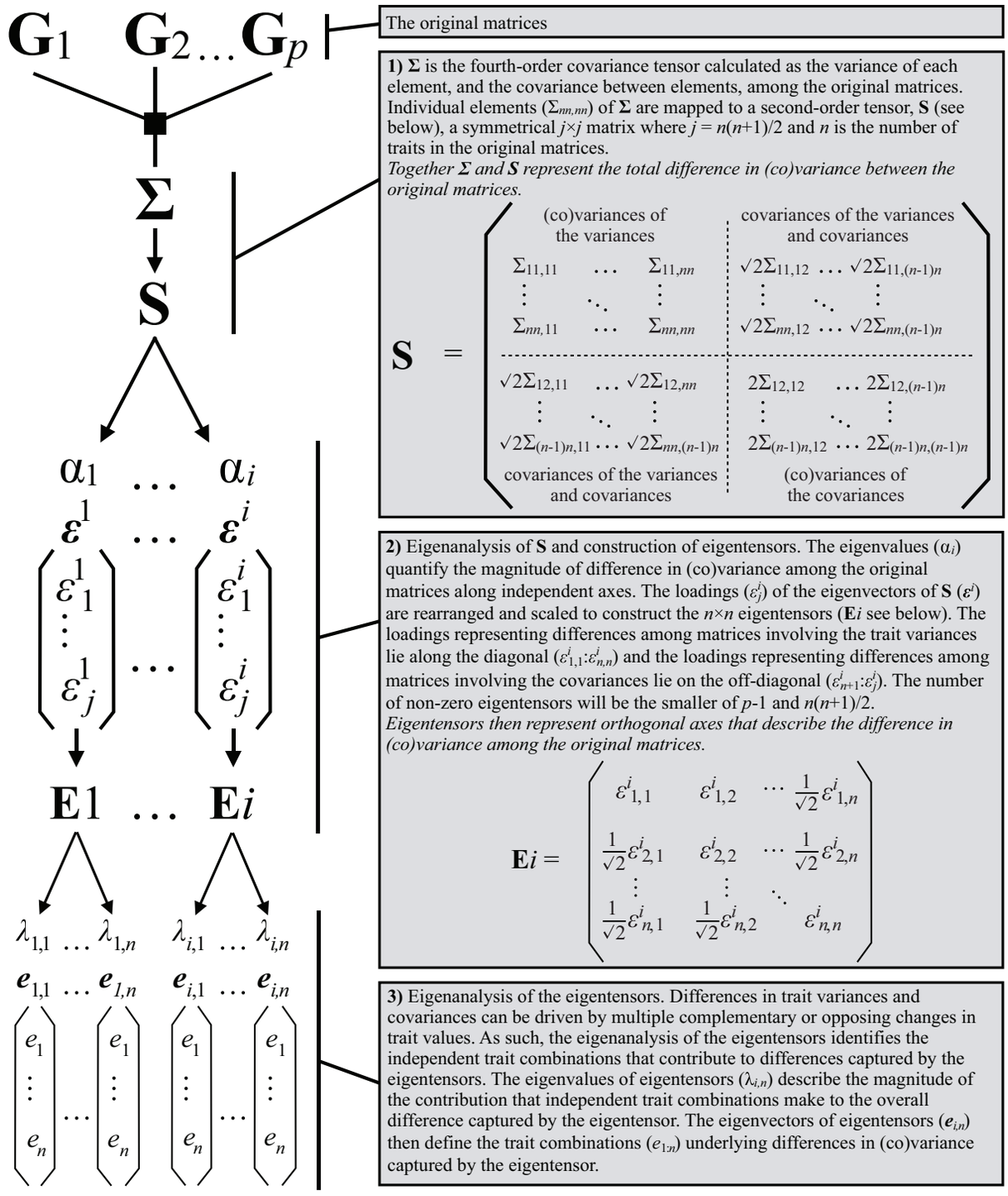

Figure 2: Description of a covariance tensor on multiple matrices. The tensor analysis is a three-step process that involves constructing the **S** matrix from the variances and covariance between elements, among matrices. Eigenvectors of **S** are then used to construct the eigentensors that represent the axes of divergence between the original matrices. A second eigenanalysis of the eigentensors then describes the contribution of the original traits to each axis of divergence. For further analytical details, see R code, available online, and the tutorial in Aguirre et al. (2014*b*).

among matrices. Not all eigentensors will have statistical support, and to determine the eigentensors associated with significant differences in genetic variation among ecotypes, we compared the magnitude of the eigenvalues of the tensor for our observed **G** with the magnitude of the eigenvalues of the tensor for our randomized **G**, following the methods described in Aguirre et al. (2014*b*). Eigenvalues of the tensor for $\mathbf{G}_{\text{null}}$ describe differences in genetic variance among matrices created by sampling error and statistical uncertainty, whereas the eigenvalues of the tensor for $\mathbf{G}_{\text{obs}}$ describe divergence in genetic variation among ecotypes. Where the eigenvalues of the tensor on $\mathbf{G}_{\text{obs}}$ exceeded the 95% HPD intervals of the distribution of posterior mean eigenvalues of the tensor on $\mathbf{G}_{\text{null}}$ was interpreted as an eigentensor that accounted for significant differences in genetic variation between ecotype matrices.

Once we quantified the differences in genetic variance among matrices using the eigentensors, we used a sequence of three steps to describe how the original matrices and traits contributed to the differences in genetic variance among matrices described by the tensor. First, the contribution of each matrix to a space describing a difference in genetic variance among matrices (the eigentensors, **E**) is defined by its coordinates (*C*) and is calculated as the Frobenius product of the original matrix and the eigentensor. Matrices with the largest absolute values of the coordinates contribute more strongly to the difference among matrices described by an eigentensor, and matrices with opposing signs contribute in opposing directions.

Second, to examine which traits contributed the most to differences among matrices we decomposed the eigenvalues and eigenvectors of the eigentensors, with an interpretation identical to that of the eigenanalysis of **C** in the two-matrix example above. The eigenvectors of an eigentensor describe the orthogonal axes of difference in variance represented by the eigentensor, with the associated eigenvalue representing the magnitude of the difference in variance. It is important to note that while eigenvectors of the same eigentensor are orthogonal, eigenvectors of different eigentensors are not constrained to orthogonality, and therefore the same trait combinations (eigenvectors of eigentensors) can contribute to more than one independent aspect of difference among matrices (eigentensors). Finally, to identify how the linear combinations of traits describing the greatest divergence in genetic variance (eigenvectors of eigentensors) differed among ecotypes, we projected the leading eigenvector of the first eigentensor ($\boldsymbol{e}_{1,1}$) through the original **G** matrices. In contrast to the coordinates of eigentensors, which represent the entire eigentensor (multiple trait axes), the eigenvectors of eigentensors represent individual axes of multivariate trait divergence. Therefore, greater values of the projection indicated ecotypes that contained more genetic variation in the direction of divergence.

Aligning Divergence in Phenotype Mean with Divergence in Genetic Variance

The matrix **D** summarizes the major axes of divergence in mean phenotype, and **E**1 summarizes the major axes of divergence in genetic variance. Therefore, if eigentensors of **G** described more variation in phenotypic divergence than expected by chance, then there is evidence that ecotypic divergence in genetic variance aligned with ecotypic divergence in phenotype mean. To investigate this, we projected the eigenvectors of the eigentensors of interest (from the tensor analysis on **G**) through **D** using

$$V_i = \boldsymbol{e}_{1,i}^{\mathrm{T}} \mathbf{D} \boldsymbol{e}_{1,i}, \tag{4}$$

where $\boldsymbol{e}_{1,i}$ is the *i*th normalized eigenvector of the first eigentensor and **D** is the divergence matrix. The value V_i is then the amount of divergence in mean phenotype associated with each eigenvector from the first eigentensor of **G**. For example, V_1 represents the amount of divergence in phenotype mean associated with the divergence in genetic variance described by $\boldsymbol{e}_{1,1}$. To carry through the uncertainty for both **G** and **D**, we implemented equation (4) on the 1,000 randomizations of **D** and the 1,000 posterior samples of the first eigentensor of **G**. If V_i explained more phenotypic divergence than expected by chance, the observed projection would fall outside the 95% confidence intervals of the null distribution, providing evidence for a strong association between divergence in genetic variance and divergence in phenotypic mean between ecotypes.

Results

Divergence in Multivariate Mean Phenotype

The four ecotypes displayed visually striking differences in leaf morphology (fig. 3*A*) and plant architecture (fig. 3*B*) under common garden conditions, suggesting a strong association between morphology and habitat. A MANOVA indicated that there was significantly more variation among ecotypes than could be accounted for by variation within ecotypes (Wilks' $\lambda = 1.09 \times 10^{-04}$, $F_{3,12} = 6.76$, $P = .002$). Multivariate phenotypic divergence among ecotypes explained much more of the total variance (62%) than divergence between populations within ecotypes (11%), highlighting a strong and consistent pattern of ecotypic divergence. From the MANOVA we calculated the phenotypic divergence matrix (**D**) of population means, which described divergence between ecotypes in multivariate space (Lande 1979; McGuigan et al. 2005; McGuigan 2006). The first eigenvector of **D** ($\boldsymbol{d}_{\text{max}}$) explained 67% of the divergence in multivariate mean phenotype, characterized by differences in traits relating to plant size in one direction and leaf shape in the other direction

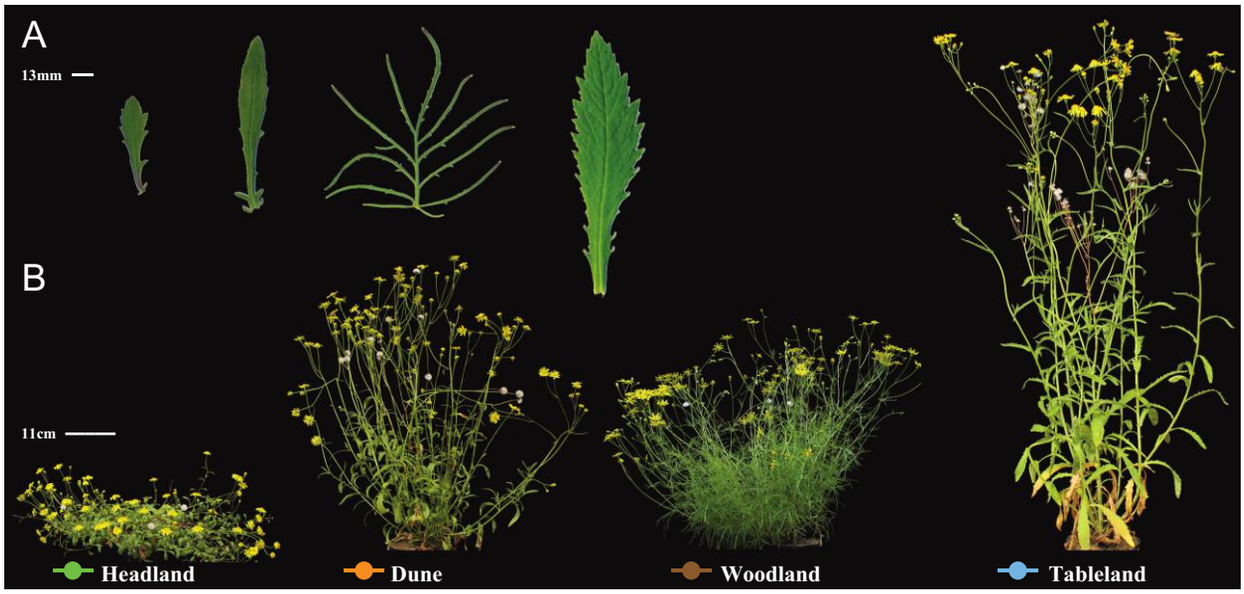

C

	Eigenvalues (proportion of variance)	5.309 (0.67)	2.497 (0.32)	0.209 (0.03)
	Eigenvectors	d_{max}	d_2	d_3
1	Height	**-0.33**	**-0.34**	**-0.36**
2	Stem length / width	**-0.36**	-0.24	-0.08
3	Number of branches	**-0.29**	**-0.29**	**0.72**
4	Stem diameter	**-0.38**	**-0.35**	-0.11
5	Leaf area	**-0.37**	-0.12	-0.18
6	Perimeter² / area²	**0.25**	**-0.41**	**0.26**
7	Circularity	**-0.31**	**0.40**	**-0.25**
8	Number of indents	**-0.33**	**0.29**	**0.30**
9	Indent width	**0.31**	-0.23	-0.20
10	Indent depth	0.16	**-0.37**	-0.21

Trait

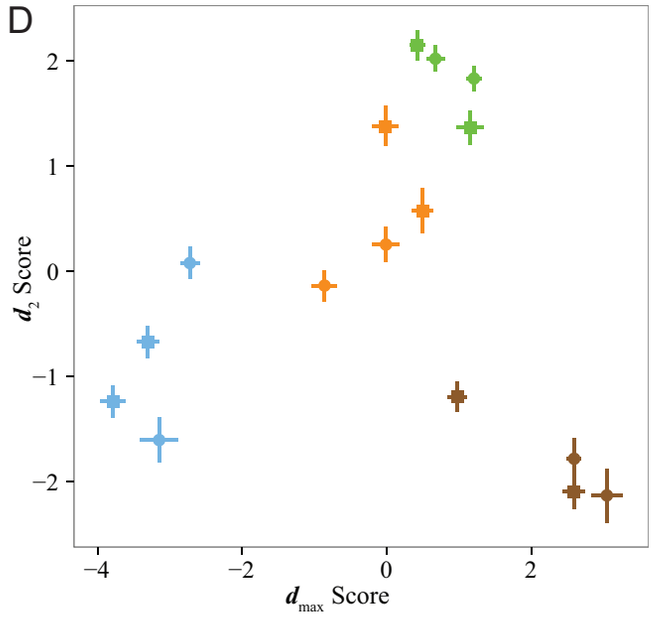

Figure 3: Ecotypes show strong differences in leaf morphology (*A*) and plant architecture (*B*). *C*, Eigenanalysis of **D** showed that multivariate divergence in mean occurred in two major axes characterized by different combinations of plant architecture and leaf traits. Numbers in boldface represent trait loadings greater than 0.25 to help interpretation. *D*, The score for each population calculated from the eigenanalysis of **D** showed that populations from the same ecotype group together. The first eigenvector separated tableland and woodland from the remaining ecotypes, while the second eigenvector separated dune and headland from the remaining ecotypes. Squares represent the populations that were used in experiment 2 to estimate **G**. Panels *A* and *B* are reproduced from Walter et al. (2016) with permission of the authors.

(fig. 3*C*), and revealed strong differences between the tableland and woodland ecotypes (fig. 3*D*). The second vector ($\boldsymbol{d}_2$) explained 32% of the variation, created by plant size and leaf complexity in one direction and number of indents and leaf circularity in the other direction (fig. 3*C*), and separated the headland and dune from the other ecotypes (fig. 3*D*). The third eigenvector ($\boldsymbol{d}_3$) explained only 3% of divergence among ecotypes (fig. 3*C*) and was primarily associated with the number of branches.

Genetic Variance Underlying Plant Morphology

Many of the observed heritabilities for univariate traits exceeded the magnitude of sampling error in our data, al-

though there was considerable variation in the magnitude of heritability among ecotypes (fig. 4). For example, the headland ecotype displayed high ($h^2 > 0.4$) and significant heritabilities for architecture traits and leaf area, while the same traits in the woodland ecotype had lower heritabilities, some of which did not exceed sampling error (fig. 4).

Genetic correlations tended to be positive among architecture traits but negative among leaf shape traits (table S1; tables S1–S3 are available online). Genetic correlations between leaf and architecture traits tended to be negative. Overall, genetic correlations were relatively weak for the dune, woodland, and tableland ecotypes (table S1), which was also reflected in the uniform distribution of genetic variance across eigenvectors and the low proportion of genetic variance accounted for by the leading eigenvector of their respective **G** matrix. The headland ecotype was the only ecotype where genetic correlations were consistently high (table S1) and where $\boldsymbol{g}_{max}$ accounted for greater than 50% of the total genetic variance (table 1; fig. 5).

Visual inspection of the eigenvectors (table 1) suggested a pattern consistent with the observed trait heritabilities, where $\boldsymbol{g}_{max}$ possessed greater loadings for architectural traits, while linear combinations of leaf traits described a small amount of genetic variance (table 1). The woodland ecotype was atypical, as both architectural and leaf traits were represented in eigenvectors containing both high and low genetic variance, and trait heritabilities were consistently low.

Divergence in Multivariate Genetic Variance among Ecotypes

To compare differences in **G** among ecotypes, we used the genetic covariance tensor, which identified the axes that

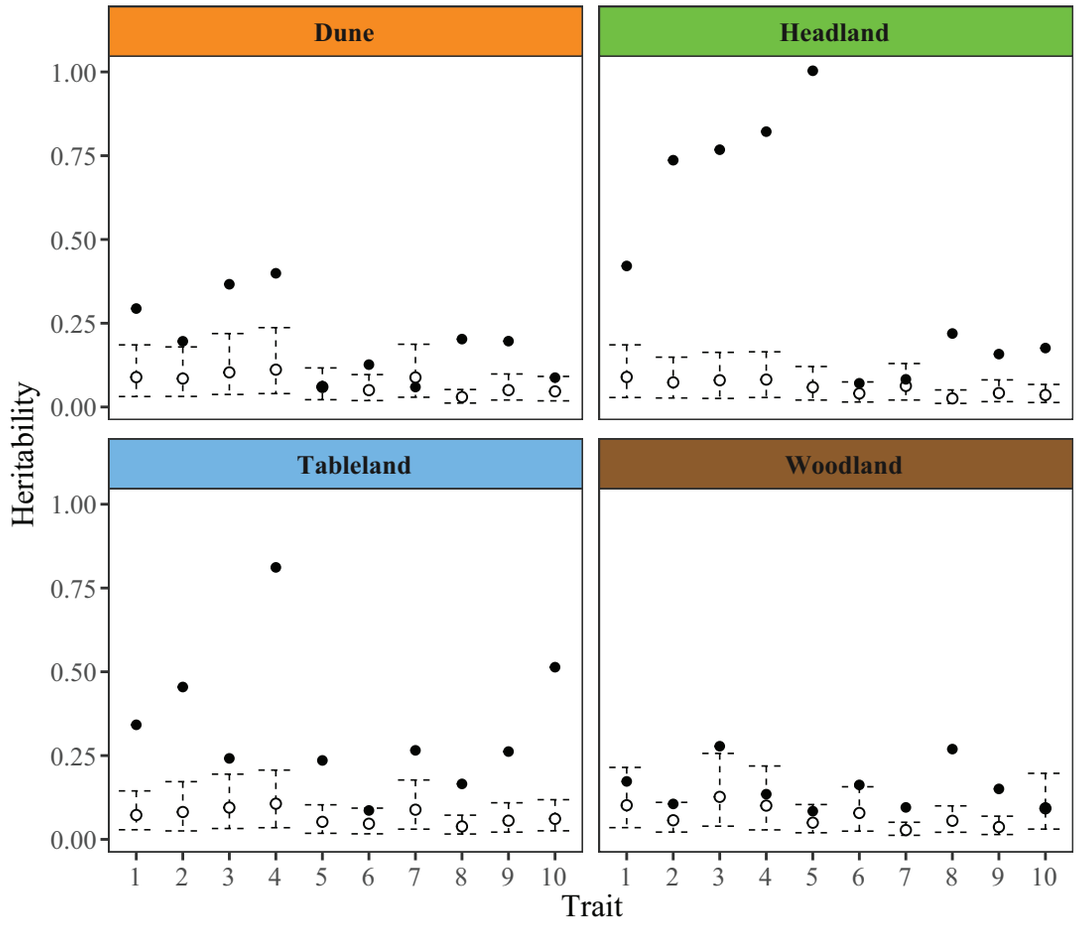

Figure 4: Observed heritabilities (filled circles) compared to the distribution of randomly estimated heritabilities (open circles). Dashed lines represent 95% highest posterior density intervals. Architecture traits showed high heritabilities in the headland and tableland, while heritabilities for all traits were lower in the dune and woodland ecotypes. Traits: 1 = height; 2 = stem length/width; 3 = number of branches; 4 = stem diameter; 5 = leaf area; 6 = perimeter^2/area^2; 7 = circularity; 8 = number of indents; 9 = indent width; 10 = indent depth.

Table 1: Eigenanalysis of the **G** matrix for each ecotype

	g_{max}	g_2	g_3	g_4	g_5	g_6	g_7	g_8	g_9	g_{10}	g_{max}	g_2	g_3	g_4	g_5	g_6	g_7	g_8	g_9	g_{10}
	Dune										Headland									
λ	.48	.39	.35	.27	.15	.11	.08	.05	.05	.04	2.22	.89	.36	.27	.26	.19	.11	.06	.05	.04
HPD	.02, 1.36	.01, .86	.00, 1.04	.03, .68	.01, .37	.01, .28	.00, .20	.00, .18	.00, .12	.00, .09	.95, 3.86	.01, 2.02	.07, .76	.06, .54	.03, .61	.01, .52	.01, .25	.01, .17	.01, .10	.00, .11
Proportion	.24	.20	.18	.14	.08	.06	.04	.03	.03	.02	.50	.20	.08	.06	.06	.04	.02	.01	.01	.01
Traits:																				
1	**−.55**	.03	−.08	**.61**	**−.46**	**−.32**	−.06	.00	−.03	.02	**−.26**	.15	**−.43**	**.37**	**.74**	−.14	−.02	.09	.05	−.11
2	**−.30**	.12	−.02	**.46**	**.53**	**.63**	−.01	−.06	.06	.02	**−.42**	**−.42**	**.36**	**−.54**	**.44**	.14	−.04	.03	.01	−.05
3	**−.52**	**.57**	**.39**	**−.40**	.21	−.22	−.02	.04	.01	−.02	.07	**−.88**	−.21	**.35**	−.12	−.15	.05	−.01	−.03	−.01
4	**−.53**	**−.78**	.06	**−.31**	.13	.02	.01	.03	.03	−.01	**−.52**	.02	**−.63**	**−.35**	**−.41**	−.04	−.16	.08	.07	−.01
5	−.04	.02	−.09	.03	.05	.02	**.49**	**.38**	**−.56**	**−.54**	**−.61**	.07	**.41**	**.55**	**−.27**	.18	−.12	.11	.09	−.11
6	.14	−.12	−.01	.22	**.54**	**−.51**	**−.50**	−.07	−.22	**−.26**	.06	.01	−.01	−.09	−.08	−.01	**.46**	.15	**.15**	**−.85**
7	−.06	.01	−.07	−.07	.00	−.02	.24	**−.86**	**−.43**	.06	−.09	.02	−.08	.04	.02	.18	−.15	**−.84**	**−.36**	**−.31**
8	−.16	.15	**−.62**	**−.25**	−.03	.12	**−.36**	.21	**−.42**	**.36**	.23	−.08	−.12	.03	.06	**.51**	**−.36**	−.11	**.72**	−.08
9	.09	−.09	**.63**	.06	**−.27**	**.31**	**−.38**	.08	**−.50**	.09	−.01	.03	.22	−.07	−.03	**−.78**	**−.35**	**−.24**	**.38**	−.15
10	.10	−.09	.19	.19	**.28**	**−.29**	**.41**	.23	−.19	**.71**	−.21	.03	−.01	.01	−.01	−.05	**.69**	**−.43**	**.42**	**.36**
	Tableland										Woodland									
λ	1.07	.87	.35	.28	.22	.18	.15	.12	.08	.05	.40	.27	.21	.18	.13	.11	.08	.07	.06	.04
HPD	.02, 2.45	.05, 1.99	.02, .84	.03, .71	.02, .58	.02, .41	.01, .36	.01, .31	.01, .19	.01, .12	.02, 1.04	.02, .72	.01, .55	.01, .45	.01, .33	.01, .30	.01, .19	.01, .17	.01, .14	.01, .10
Proportion	.32	.26	.10	.08	.06	.05	.04	.04	.02	.02	.26	.17	.14	.12	.08	.07	.05	.04	.04	.03
Traits:																				
1	**−.39**	−.09	**−.34**	−.18	**.28**	**.75**	−.18	.02	.12	.03	.13	.01	**.56**	**.57**	**.55**	.11	.15	−.06	−.01	−.07
2	**−.48**	.18	**−.48**	**−.29**	.23	**−.54**	**.27**	.08	.00	−.02	.10	.23	.23	.24	−.22	**−.37**	**−.53**	**.51**	**−.29**	.14
3	.00	−.13	**−.32**	**−.32**	**−.84**	.12	.10	.13	−.16	.01	**−.49**	**.72**	.33	**−.31**	.06	.08	.08	.01	.13	.05
4	**−.71**	**−.47**	**.37**	**.30**	−.20	−.11	−.02	−.04	.02	.00	−.14	−.17	**.39**	.16	**−.57**	**−.44**	**.46**	−.17	.09	−.02
5	−.15	**.34**	.16	−.23	−.16	.02	−.03	**−.78**	.11	**.37**	.01	**−.29**	.23	−.08	−.02	.13	−.22	.20	**.70**	**.51**
6	.07	−.01	.03	.08	−.06	.02	**.28**	**.36**	**.59**	**.66**	**.36**	**.29**	−.22	−.08	**.33**	**−.68**	.06	−.14	**.37**	.01
7	−.15	**.36**	.09	−.11	−.17	−.19	**−.78**	**.32**	.22	−.01	.01	**−.25**	**.31**	**−.36**	.08	−.09	−.21	.21	.20	**−.75**
8	.02	−.21	.24	**−.40**	.22	−.05	−.14	.20	**−.59**	**.53**	**−.68**	−.11	**−.38**	**.45**	.14	−.18	−.08	.17	.24	−.18
9	.09	−.15	**−.56**	**.56**	−.02	−.14	**−.33**	−.19	−.20	**.37**	**.27**	**.37**	−.10	**.38**	**−.42**	**.32**	−.21	−.20	**.39**	**−.33**
10	**−.25**	**.64**	.10	**.39**	−.11	.24	.24	.24	**−.41**	.10	.22	.12	−.16	.04	−.04	.15	**.58**	**.73**	.11	−.08

Note: Eigenvectors are columns, and the first four rows show the associated eigenvalues (λ) with their upper and lower 95% HPD intervals and the proportion of genetic variance they described. The remaining rows show the trait loadings, where numbers in boldface denote trait loadings greater than 0.25 to aid interpretation. Architecture traits contributed to the genetic variance contained in g_{max} for all ecotypes except the woodland. Leaf shape traits were represented only in eigenvectors with low genetic variance. Traits: 1 = plant height; 2 = stem length/width; 3 = number of branches; 4 = stem diameter; 5 = leaf area; 6 = perimeter^2/area^2; 7 = circularity; 8 = number of indents; 9 = indent width; 10 = indent depth. HPD = highest posterior density.

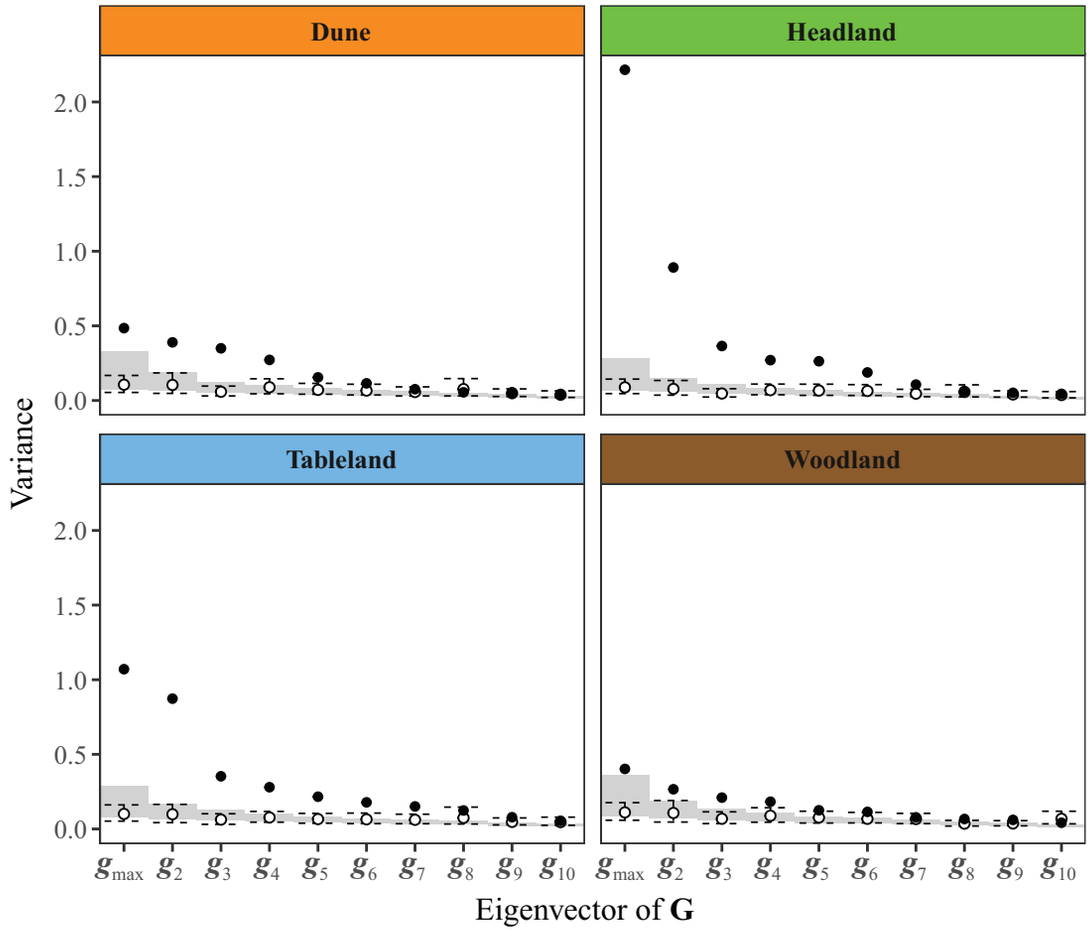

Figure 5: Observed eigenvalues of **G** (filled circles) compared to the distribution of random eigenvalues of **G** (gray bars represent 95% highest posterior density [HPD] intervals). The headland was the only ecotype that showed a much greater amount of variance in $\boldsymbol{g}_{max}$, while the remaining ecotypes exhibited a similar partitioning of genetic variance among eigenvectors. Open circles and dashed lines (95% HPD intervals) represent the genetic variance in $\mathbf{G}_{null}$ described by the observed eigenvectors. All ecotypes showed at least four eigenvectors with greater genetic variance than expected by chance.

described the major differences in genetic variance underlying architecture and leaf traits. We found three significant eigentensors of **G** that explained 38%, 11%, and 7% of the divergence in genetic variance between ecotypes, respectively. All three eigentensors described more divergence in genetic variance than expected by sampling error alone (fig. S3). The coordinates of the ecotypes in the space of the eigentensor revealed how each ecotype contributed to differences in genetic variance. We were able to detect significant differences between ecotypes only in the first eigentensor (**E**1; fig. S4). We therefore concentrate our analysis on the first eigentensor (table 2), while the full tensor analysis can be found in table S2.

The first eigentensor was dominated by the first eigenvector ($\boldsymbol{e}_{1,1}$), a linear combination of plant architectural traits and leaf area that explained 62% of the divergence in genetic variance between ecotypes for **E**1 (table 2). The first three eigenvectors of **E**1 described divergence in genetic variance underlying different aspects of architecture traits and leaf area, accounting for 85% of the difference in genetic variance in **E**1. In contrast, differences in genetic variance underlying leaf shape traits ($\boldsymbol{e}_{1,4}$ and $\boldsymbol{e}_{1,7}$–$\boldsymbol{e}_{1,10}$) together represented only 8% of the difference in genetic variance between ecotypes for **E**1 (table 2).

The coordinates of the ecotype **G** matrices in the space of the first eigentensor showed that divergence in genetic variance between the headland ecotype and the dune and woodland ecotypes was responsible for the divergence in genetic variance described by the eigentensor (fig. 6*A*). We confirmed this result by projecting $\boldsymbol{e}_{1,1}$ through the original **G** matrices, which quantified the contribution of each ecotype to the major axis of divergence in genetic variance (fig. 6*B*).

Table 2: Table summary of the covariance tensor analysis of **G** for the first eigentensor that described 38% of divergence in genetic variance ($\alpha = 1.24$, HPD interval = 0.10, 2.95)

	$\boldsymbol{e}_{1,1}$	$\boldsymbol{e}_{1,2}$	$\boldsymbol{e}_{1,3}$	$\boldsymbol{e}_{1,4}$	$\boldsymbol{e}_{1,5}$	$\boldsymbol{e}_{1,6}$	$\boldsymbol{e}_{1,7}$	$\boldsymbol{e}_{1,8}$	$\boldsymbol{e}_{1,9}$	$\boldsymbol{e}_{1,10}$
λ	−.95	−.26	−.09	.08	−.07	−.04	.02	.02	.00	.00
Proportion	(.62)	(.17)	(.06)	(.05)	(.04)	(.03)	(.02)	(.01)	(.00)	(.00)
Traits:										
1	**−.25**	.23	**.44**	.00	.09	**.74**	−.14	.03	.14	**.30**
2	**−.45**	**−.51**	−.05	.03	**−.71**	.07	−.13	−.06	.06	.03
3	.04	**−.81**	.10	.00	**.54**	.13	.08	.05	−.02	.09
4	**−.50**	.08	**.55**	−.20	.16	**−.59**	−.03	.08	−.04	.14
5	**−.61**	.14	**−.65**	−.17	**.36**	.08	−.10	−.11	.00	−.01
6	.07	−.02	.04	**.48**	.14	−.16	**−.75**	**−.39**	−.04	.05
7	−.09	.02	.11	.04	−.04	.13	**.27**	**−.48**	**−.81**	−.02
8	.21	−.06	.01	**−.73**	−.05	.09	**−.54**	.13	**−.29**	−.13
9	.00	.03	−.19	**.29**	−.05	−.05	−.11	**.66**	**−.45**	**.47**
10	−.23	.02	.16	**.28**	.08	.14	−.09	**.38**	−.16	**−.80**

Note: The eigenvectors ($\boldsymbol{e}_{1,1}$–$\boldsymbol{e}_{1,10}$) and λ represent the eigenanalysis of the eigentensor, giving the linear combinations of traits that describe the difference in the eigentensor. The λ value describes the amount of variation in the eigentensor that each eigenvector explains (proportion of variance in parentheses), with the trait loadings quantifying the contribution of each trait to differences in variance. Numbers in boldface denote trait loadings greater than 0.25 to aid interpretation. Plant architecture traits accounted for the greatest difference in genetic variance. Traits: 1 = plant height; 2 = stem length/width; 3 = number of branches; 4 = stem diameter; 5 = leaf area; 6 = perimeter^2/area^2; 7 = circularity; 8 = number of indents; 9 = indent width; 10 = indent depth. HPD = highest posterior density.

Therefore, the headland ecotype has diverged the most from the other ecotypes in genetic variance for plant architecture and leaf area.

Aligning Divergence in Phenotype Mean with Divergence in Genetic Variance

The overarching goal of our study was to investigate whether phenotypic divergence was associated with divergence in genetic variance, which is analogous to examining whether the major axis of divergence in genetic variance ($\boldsymbol{e}_{1,1}$) is associated with divergence in mean phenotype, **D**. Projection of eigenvectors from the first eigentensor of **G** ($\boldsymbol{e}_{1,1}$–$\boldsymbol{e}_{1,10}$) through **D** quantified how much divergence in mean phenotype was associated with each eigenvector that represented divergence in genetic variance. If eigenvectors that described a large amount of divergence in genetic variance also described a large amount of phenotypic divergence, then we took this as evidence for changes in genetic variance aligning with changes in phenotype mean. We found that the $\boldsymbol{e}_{1,1}$ trait combination described greater divergence in mean than expected by chance (fig. 7), suggesting that substantial divergence in genetic variance underlying plant architecture traits was associated with divergence in phenotypic mean. However, two eigenvectors associated with divergence in genetic variance underlying leaf shape traits ($\boldsymbol{e}_{1,4}$ and $\boldsymbol{e}_{1,8}$) also described a large amount of divergence in phenotypic mean, suggesting that small genetic changes underlying leaf morphology traits were also associated with phenotypic divergence.

Given that $\boldsymbol{e}_{1,1}$ and $\boldsymbol{e}_{1,4}$ described large and significant variance in phenotypic divergence, we then asked whether these two axes of divergence in genetic variance were both associated with the largest axis of divergence in mean phenotype ($\boldsymbol{d}_{\max}$). Since $\boldsymbol{e}_{1,1}$ and $\boldsymbol{e}_{1,4}$ were orthogonal, we calculated the vector that bisected these two vectors using $\boldsymbol{b} = (\boldsymbol{e}_{1,1} + \boldsymbol{e}_{1,4})/2$ and normalized $\boldsymbol{b}$ to unit length. If $\boldsymbol{b}$ was similar to $\boldsymbol{d}_{\max}$, then there is evidence that phenotypic divergence along $\boldsymbol{d}_{\max}$ required a coordinated genetic change along two different axes of genetic variance. We found a vector correlation between $\boldsymbol{b}$ to $\boldsymbol{d}_{\max}$ of 0.85, suggesting a close alignment between the vector representing divergence along two axes of genetic divergence and the vector describing the greatest divergence in phenotype mean (see fig. S5 for a vector diagram).

Adaptation is expected to be biased by the line of greatest genetic variance ($\boldsymbol{g}_{\max}$; Schluter 1996), but $\boldsymbol{g}_{\max}$ itself might change during the early stages of adaptive divergence if natural selection or genetic drift change allele frequencies in genes underlying trait variation. If $\boldsymbol{g}_{\max}$ can align with the direction of natural selection during the early stages of adaptation, then natural selection along the axis with the highest genetic variation can facilitate rapid divergence to create adaptive radiation (Eroukhmanoff 2009).

Eigentensors describe differences in genetic variance for the entire multivariate space under consideration. Therefore, eigentensors do not distinguish differences in the orientation of **G** but simply which ecotypes differed the most in multivariate genetic space. Plant architecture and leaf morphology trait loadings for $\boldsymbol{g}_{\max}$ were different between

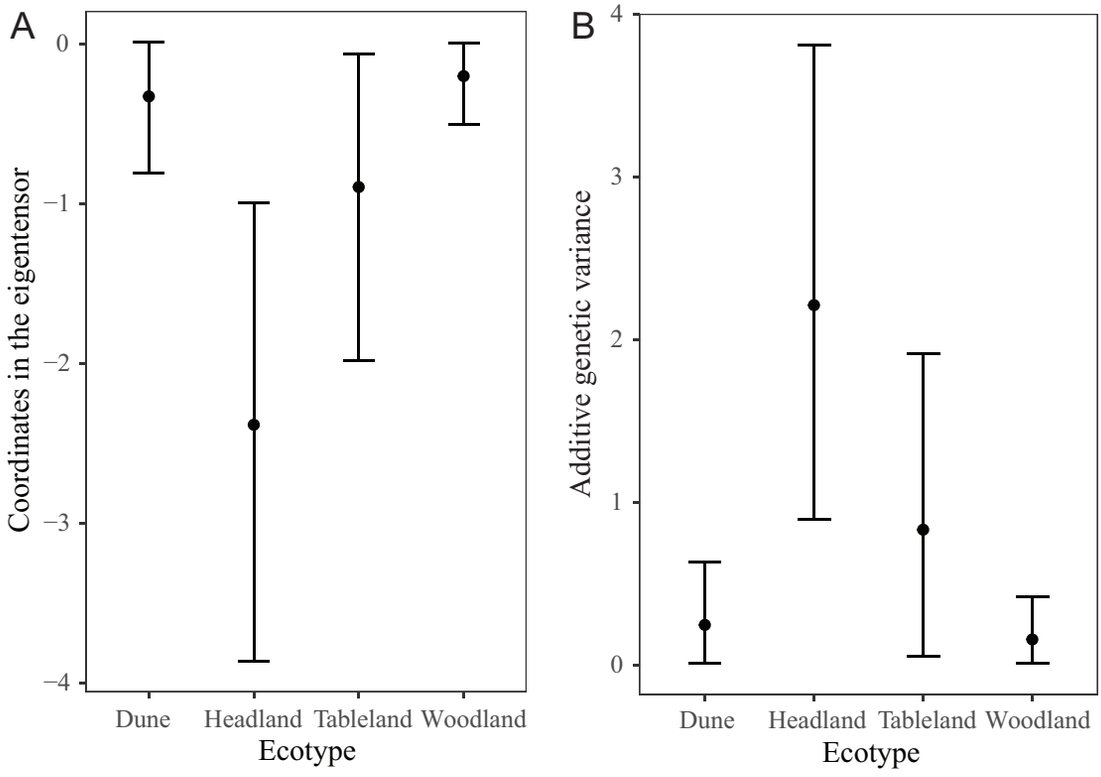

Figure 6: *A*, Mean and 95% highest posterior density (HPD) intervals for the coordinates of each ecotype **G** matrix in the space of the first eigentensor (**E**1) of **G**. *B*, Mean and 95% HPD intervals for the projection of the leading eigenvector from the first eigentensor of **G** through the original ecotype **G** matrices. The headland ecotype showed strong divergence in additive genetic variance from the dune and woodland ecotypes.

ecotypes (table 1), suggesting that $\boldsymbol{g}_{\max}$ has diverged in orientation during adaptive divergence. To identify whether changes in the orientation of **G** aligned with divergence in phenotype mean, we quantified the alignment between divergence in $\boldsymbol{g}_{\max}$ and $\boldsymbol{g}_2$ and divergence in phenotype mean. The analytical process was similar to projecting the eigenvectors of eigentensors of **G** through **D** (fig. 7), but rather than comparing the entire space of **G** among ecotypes, here we focus only on differences in the orientation of $\boldsymbol{g}_{\max}$ and $\boldsymbol{g}_2$. First, we converted $\boldsymbol{g}_{\max}$ and $\boldsymbol{g}_2$ for each ecotype into covariance matrices using $\mathbf{C}_{ij} = \boldsymbol{A}_{ij}\boldsymbol{A}_{ij}^{\mathrm{T}}$, where $\boldsymbol{A}_{ij}$ represents the *i*th vector of **G** ($\boldsymbol{g}_{\max}$ or $\boldsymbol{g}_2$) for the *j*th ecotype. We then used the tensor approach to quantify differences in $\mathbf{C}_{\boldsymbol{g}_{\max}}$ and $\mathbf{C}_{\boldsymbol{g}_2}$ among ecotypes. Here, the eigentensors represented ecotypic divergence in the orientation of the major axes of genetic variation. Projection of the eigenvectors from the first eigentensor ($\boldsymbol{e}_{1,1}$–$\boldsymbol{e}_{1,10}$) of $\mathbf{C}_{\boldsymbol{g}_{\max}}$ and $\mathbf{C}_{\boldsymbol{g}_2}$ through **D** quantified the alignment between divergence in the orientation of major axes of **G** and divergence in phenotype mean.

The first eigentensor of both tensor analyses captured large differences between ecotypes for both $\mathbf{C}_{\boldsymbol{g}_{\max}}$ and $\mathbf{C}_{\boldsymbol{g}_2}$, where **E**1 described 56% of divergence in the orientation of $\boldsymbol{g}_{\max}$ and 48% of divergence in the orientation of $\boldsymbol{g}_2$. The corresponding eigenvectors of eigentensors represented the axes of greatest divergence in the orientation of $\boldsymbol{g}_{\max}$ and $\boldsymbol{g}_2$ among ecotypes. The first two eigenvectors of **E**1 ($\boldsymbol{e}_{1,1}$ and $\boldsymbol{e}_{1,2}$) for $\boldsymbol{g}_{\max}$ and $\boldsymbol{g}_2$ described most of the difference in variance explained by the first eigentensor ($\boldsymbol{g}_{\max}\boldsymbol{e}_{1,1} = 50\%$ and $\boldsymbol{e}_{1,2} = 46\%$; $\boldsymbol{g}_2\boldsymbol{e}_{1,1} = 50\%$ and $\boldsymbol{e}_{1,2} = 41\%$). For the full tensor analyses, see table S3.

Projection of the eigenvectors from the first eigentensor of $\mathbf{C}_{\boldsymbol{g}_{\max}}$ and $\mathbf{C}_{\boldsymbol{g}_2}$ through the observed and random **D** matrices (using eq. [4]) quantified the amount of divergence in mean phenotype associated with divergence in the orientation of the major eigenvectors of ecotype **G**. For $\boldsymbol{g}_{\max}$, both $\boldsymbol{e}_{1,1}$ and $\boldsymbol{e}_{1,2}$ accounted for more divergence in phenotype mean than expected by chance (fig. 8*A*). For $\boldsymbol{g}_2$, only eigenvectors associated with small divergence in orientation ($\boldsymbol{e}_{1,3}$, $\boldsymbol{e}_{1,4}$, and $\boldsymbol{e}_{1,6}$) described a similar amount of divergence in phenotype mean (fig. 8*B*). Therefore, strong differences in the orientation of $\boldsymbol{g}_{\max}$ but not $\boldsymbol{g}_2$ aligned with divergence in mean phenotype, suggesting that the major axis of additive genetic variance underlying plant architecture and leaf morphology has diverged in orientation between

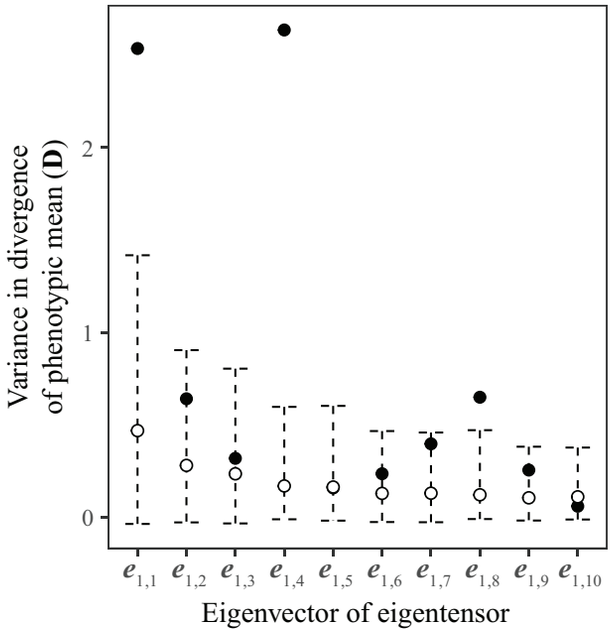

Figure 7: Projection of eigenvectors of the first eigentensor of **G** through the observed (filled circles) and randomized (open circles) **D** matrices. Dashed lines represent 95% highest posterior density intervals for the projections through the randomized **D** matrices. Eigenvector 1 showed a strong association with divergence in mean phenotype. However, eigenvectors 4 and 8 also described a large amount of variance in divergence, suggesting that small changes in genetic variance also explained large variance in divergence.

ecotypes, and this was associated with divergence in phenotype mean.

Discussion

Here, we have explored the association between divergence in multivariate phenotypic mean and divergence in genetic variance in an early radiation to investigate how adaptive radiation may proceed. A key component of our experimental design is the use of replicate populations of each ecotype. Partitioning the multivariate phenotypic variation to isolate the variation associated with ecotype (**D**), rather than replicate populations within ecotypes, quantified the divergence correlated with the environment and hence implies that selection rather than genetic drift is the likely causal agent of this divergence. Unfortunately, this strength of our experimental design was not paralleled in our estimate of **G** for each ecotype, where a single **G** was estimated from the combined data from replicate populations within each ecotype. The variation among **G** matrices we report, interpreted in isolation, could therefore be a consequence of either drift or selection. However, the main purpose of our analysis was to associate divergence in mean with divergence in genetic variance. By using the major axes of **D** to interrogate the changes in genetic variance, we can associate those changes in the distribution of genetic variance that are consistent with the action of selection.

Multivariate Divergence in Mean Phenotype and Genetic Variance among Ecotypes

Multivariate phenotypic divergence was stronger between ecotypes than within ecotypes, indicating that environment-specific phenotypes have arisen due to similar natural selection regimes in populations that share similar habitats (Langerhans 2010; Rosenblum and Harmon 2011). Phenotypic divergence was very strong in two axes, separating tableland and woodland ecotypes from the dune and headland ecotypes in one axis and dune and headland from the tableland and woodland ecotypes in the second axis (fig. 3). Additional evidence for natural selection creating divergence comes from the repeated and independent evolution of parapatric pairs of dune and headland populations along the coastline, with pairs separated tens to hundreds of kilometers (Roda et al. 2013*a*, 2013*b*; Melo-Hurtado 2014). These patterns of replicated evolution across a large geographical scale are similar to those documented in sticklebacks (Colosimo et al. 2005), African cichlids (Muschick et al. 2012), and *Anolis* lizards (Langerhans et al. 2006).

We observed divergence in the amount of additive genetic variation where plant architecture traits generally had greater heritabilities than leaf traits. However, this was ecotype dependent, suggesting divergence in the amount of additive genetic variance underlying the same traits. The tensor analysis on **G** quantified divergence in the distribution of additive genetic variation, where one major axis of divergence was represented by plant architecture traits, while divergence in genetic variance underlying leaf morphology traits was very low. More specifically, the distribution of genetic variation in the headland ecotype was dramatically different to the remaining ecotypes, with greater levels of genetic variance concentrated into a few trait combinations represented by plant architecture traits. Therefore, ecotypes that occupy contrasting environments were associated with divergence in plant architecture and leaf morphology traits, as well as divergence in the genetic variance underlying these traits.

The tableland and headland ecotypes showed greater trait heritabilities and greater genetic variance in linear combinations of architecture traits, which was reflected by contrasting architectural phenotypes. Plant architecture for the tableland ecotype was similar to the dune and woodland ecotypes but more extreme in terms of overall plant size, potentially due to selection for larger plant size in a rainforest environment (Dudley and Schmitt 1995; Ackerly et al. 2000; Reich 2014). Therefore, it is possible that natural selection along genetic pathways common to the dune, woodland, and table-

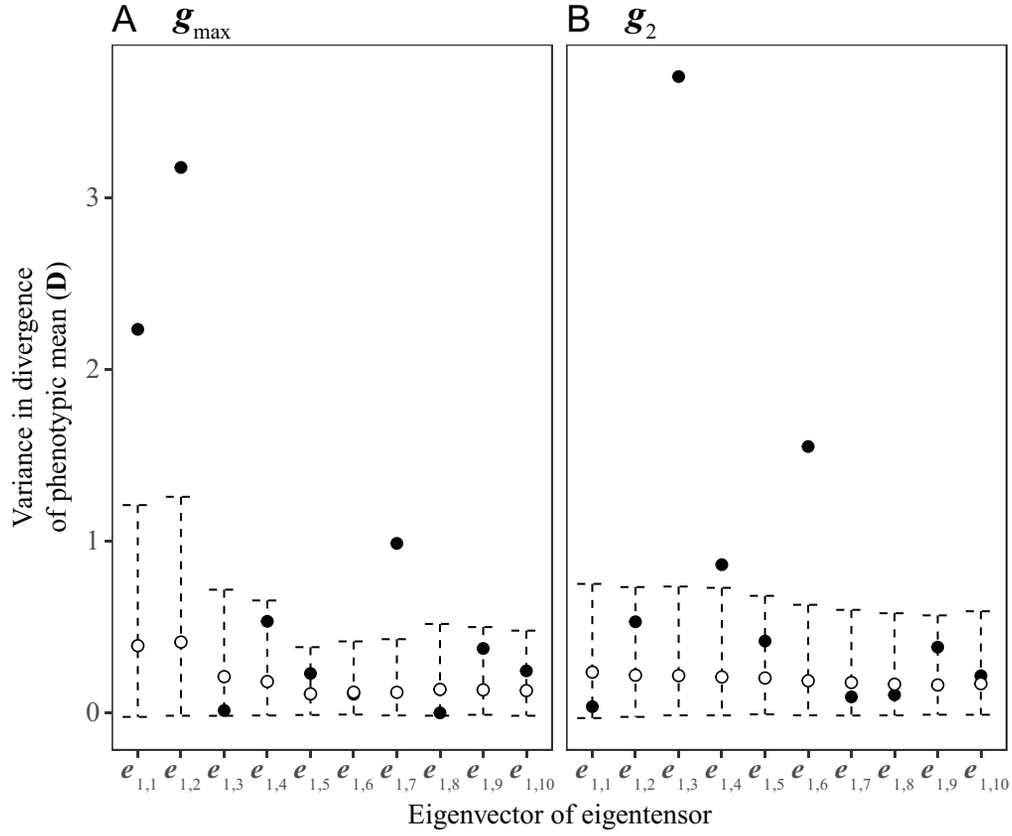

Figure 8: Projection of eigenvectors from the first eigentensor taken from tensor analyses conducted on $\mathbf{C}_{g_{max}}$ (*A*) and $\mathbf{C}_{g_2}$ (*B*), through the observed (filled circles) and random (open circles) **D** matrices. Confidence intervals represent 95% highest posterior density intervals for the projection through the random **D** matrices. Divergence in the orientation of $\boldsymbol{g}_{max}$ but not $\boldsymbol{g}_2$ described strong divergence in mean phenotype.

land ecotypes might have created larger plants in the tableland environment. The prostrate form of the headland ecotype is especially contrasting to the other ecotypes and is typical of many plants occupying exposed environments subject to strong winds (Foster et al. 2007; Lowry et al. 2008*b*). Highly diverged genetic variance underlying the highly diverged plant architecture in the headland ecotype suggests that strong differences in natural selection might have used large genetic changes to create the prostrate phenotype beneficial in the headland environment.

A recent study on the genetic basis of the prostrate phenotype in *Senecio lautus* found that a quantitative trait locus controlled substantial levels of variation in plant height, number of branches, and the angle of the stem (Roda et al. 2017), suggesting that pleiotropic effects might be partly responsible for the evolution of the prostrate growth habit in the system. In other coastal systems, such as *Mimulus guttatus* ecotypes from California, a chromosomal inversion affects multiple traits and fitness, consistent with the idea that the genetic basis of adaptation might require at least some loci that dramatically change the morphology of the plant (Lowry et al. 2008*a*). Whether such loci segregated as rare alleles in the population before colonization of a new habitat remains an open question for future studies of adaptation (but see Barrett et al. 2008).

Aligning Divergence in Phenotype Mean with Divergence in Genetic Variance

During the initial stages of adaptive divergence, the association between the direction of natural selection on multivariate phenotypes and the distribution of genetic variance is expected to determine evolutionary trajectories. However, over long periods of time, the direction of selection alone is expected to dominate adaptive divergence between habitats, regardless of the underlying genetic architecture (Zeng 1988; Schluter 1996). In our experiment, the presence of strong divergence in **G** following a recent radiation argues against making an implicit assumption that genetic correlations maintain a stable ancestral **G** matrix and its influence on divergence in phenotype during the early stages of diversification. Our results are consistent with several studies that

found differences in **G** following very recent divergence (Doroszuk et al. 2008; Eroukhmanoff and Svensson 2011; Wood and Brodie 2015), suggesting that rapid adaptive divergence may occur when the colonization of novel environments occurs and natural selection changes the mean phenotype, as well as the distribution of underlying genetic variance.

The tensor analysis of **G** showed divergence in the distribution of additive genetic variance among ecotypes. Different beneficial alleles in each environment may have increased in frequency, changing the shape and orientation of **G** among ecotypes. The axis of greatest divergence in genetic variance ($\boldsymbol{e}_{1,1}$) was associated with divergence in phenotype mean, suggesting that the changes in genetic variance, created by changes in allele frequency, were associated with adaptive evolution represented by consistent divergence in phenotype mean among ecotypes. Furthermore, the axis of greatest divergence in phenotype mean ($\boldsymbol{d}_{\max}$) aligned with two orthogonal vectors of divergence in genetic variance ($\boldsymbol{e}_{1,1}$ and $\boldsymbol{e}_{1,4}$), suggesting that a coordinated change along two different axes of genetic variance were required to reach the contrasting phenotypes observed. Given that $\boldsymbol{e}_{1,1}$ represented divergence in genetic variance underlying plant architecture and $\boldsymbol{e}_{1,4}$ leaf morphology, we suggest that leaf and plant architecture traits might evolve independently, where genetically correlated traits evolve as a module (e.g., architecture traits) that can evolve rapidly and independently of other trait modules (Melo and Marroig 2015). Therefore, our results provide evidence that divergent natural selection has promoted rapid adaptive divergence in phenotype via changes to the distribution of genetic variance underlying plant architecture and leaf morphology traits, independently.

We also found that changes in the orientation of $\boldsymbol{g}_{\max}$ but not the orientation of $\boldsymbol{g}_2$ were associated with changes in phenotype mean, suggesting that the linear combination of traits with the greatest genetic variance have changed orientation and aligned with phenotypic divergence. Therefore, adaptation has occurred along lines of greatest additive genetic variance, which natural selection can modify. This suggests that genetic correlations are not entirely stable and may not constrain adaptation during adaptive radiation as predicted (Schluter 1996). Perhaps the simplest explanation for finding an association between divergence in mean and divergence in the major axis of genetic variance would involve a selection response based on alleles segregating at low frequency. Under models of polygenic selection from standing genetic variation, rare alleles maintained by mutation-selection balance might contribute little to genetic variance (Turelli 1984; Zhang and Hill 2005). After colonization of a novel habitat, some of these previously rare alleles may become beneficial and rise in frequency during adaptation, contributing more substantially to levels of additive genetic variation in traits under selection. The increase in frequency of previously rare alleles would then promote the evolution of genetic correlations, changing the orientation of genetic variance (fig. 9*A*; Carriere and Roff 1995; Agrawal et al. 2001; Orr and Betancourt 2001; B. Walsh and M. Lynch, unpublished manuscript). Polygenic selection on many alleles of small effect should promote a rise in frequency but not necessarily fixation (Walsh and Blows 2009; Pritchard et al.

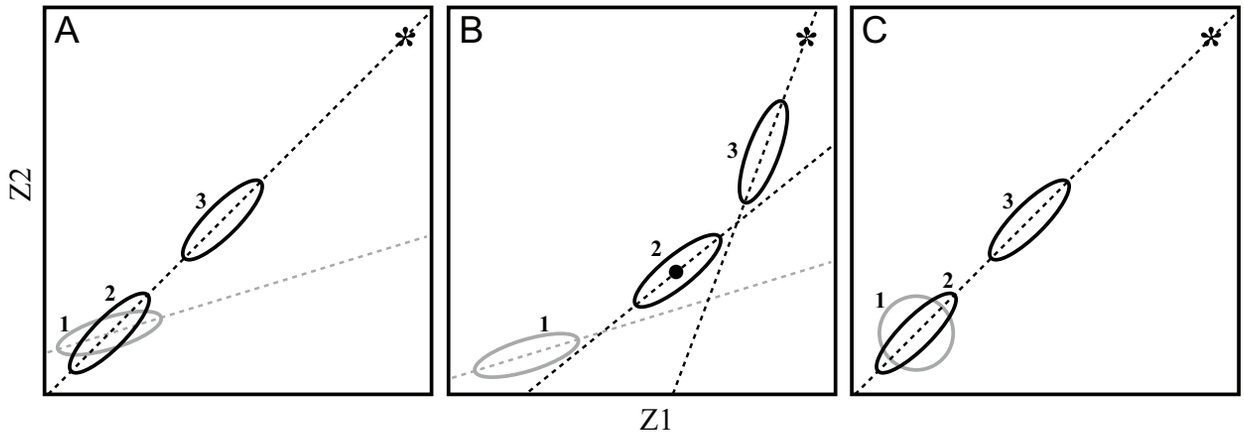

Figure 9: Evolution of **G** (ellipses with dashed lines denoting $\boldsymbol{g}_{\max}$) in two traits for one ecotype from the ancestor (gray) to derived states (black) in three steps (numbered) as the ecotype moves toward the optimum (asterisk). *A*, Evolution of genetic correlations that change the orientation of $\boldsymbol{g}_{\max}$. *B*, If genetic constraints and changes in **G** occur simultaneously, we expect adaptation to occur along $\boldsymbol{g}_{\max}$, with $\boldsymbol{g}_{\max}$ evolving concurrently. If this option is true, our experiments might have measured an intermediate stage in adaptive divergence (black circle). Further experiments showing a difference between the direction of selection and direction of evolution are required to verify the presence of genetic constraints. *C*, Ancestor with genetic variance in all directions followed by evolution of beneficial genetic correlations that create $\boldsymbol{g}_{\max}$ orientated toward the optimum.

2010). However, adaptation can occur via selection on alleles of many different effect sizes, and we expect alleles with large beneficial effects to rise to fixation, reducing genetic variation for some regions of phenotypic space (Pritchard et al. 2010). For example, leaf morphology traits showed high phenotypic divergence but very low divergence in underlying genetic variance.

Our experiments cannot identify the existence of genetic constraints, as we measured only the evolutionary outcome (change in phenotype mean) and not the direction of natural selection. Therefore, it is possible that during adaptation a balance exists between the stability and flexibility of genetic correlations, such that changes in the orientation of $\boldsymbol{g}_{max}$ may occur concurrently with genetic constraints that move the phenotype mean on a curved trajectory toward an optimum (fig. 9*B*). One final alternative exists, where the ancestral **G** possessed genetic variance in many directions in multivariate space (spherical **G**), which could facilitate the colonization of contrasting environments due to lack of genetic constraints among selected traits. Environment-specific beneficial genetic correlations could evolve as linkage disequilibrium builds or beneficial pleiotropic loci increase in frequency. This would lead to **G** matrices specific to each environment and allow rapid adaptive divergence along lines of additive genetic variance (fig. 9*C*).

Conclusions

Overall, our results suggest that during the early stages of adaptive divergence genetic correlations are either weak or can evolve via the fixation of rare alleles previously kept at low frequency by mutation-selection balance. We propose that flexibility in the genetic basis of adaptive phenotypes can promote the evolution of genetic correlations in response to directional natural selection, promoting adaptive radiation. Strong genetic constraints that bias the direction of adaptation might evolve only after the early stages of adaptive divergence when genetic correlations are strengthened, which might also explain the observed decline in diversification rate as radiations proceed.

Acknowledgments

We are very appreciative to Edmund D. Brodie III, Alice A. Winn, and two anonymous reviewers for their help in improving this article. We thank Carol Palmer, who was integral in the collection of the phenotype data. We also thank the University of Queensland glasshouse staff for their help and support. We are grateful to Tom Richards for his help with field sampling and providing comments on previous manuscripts. We also thank Jayne Walter, Federico Roda, Gail Walter, Kristylee Marr, and James Donohoe for their help with field sampling. Scott Walter provided important help in the glasshouse. Emma Hine provided insightful discussions during analysis. This project was funded by Australian Research Council grant DP0986172. Seeds were collected in New South Wales national parks under permit number S12084.

APPENDIX

SUPPLEMENTARY TABLES

Table A1: Population locations

Ecotype and population code	Latitude	Longitude	Location	Variance estimated	Mean estimated
Dune:					
D0	−27.39845	153.453808	Stradbroke Island, Queensland	No	Yes
D1	−28.783005	153.594018	Lennox Head, New South Wales	Yes	Yes
D3	−28.331043	153.571228	Cabarita Beach, New South Wales	Yes	Yes
D4	−30.31275	153.137762	Coffs Harbour, New South Wales	No	Yes
Headland:					
H0	−27.436047	153.545529	Stradbroke Island, Queensland	No	Yes
H1	−28.813117	153.605319	Lennox Head, New South Wales	Yes	Yes
H2	−28.362519	153.574345	Cabarita Beach, New South Wales	Yes	Yes
H5	−30.311827	153.145572	Coffs Harbour, New South Wales	No	Yes
Tableland:					
T1	−28.230508	153.135078	O'Reilley's Rainforest Retreat, Queensland	Yes	Yes
T5	−30.488289	152.409297	New England National Park, New South Wales	No	Yes
T9	−28.293389	152.415917	Near Queen Mary Falls, Queensland	Yes	Yes

Table A1 (*Continued*)

Ecotype and population code	Latitude	Longitude	Location	Variance estimated	Mean estimated
T13	−26.892234	151.619021	Bunya Mountains, Queensland	No	Yes
Woodland:					
W1	−31.272984	149.070783	Warrumbungles National Park, New South Wales	No	Yes
W2	−27.479946	152.824709	Upper Brookfield, Queensland	Yes	Yes
W3	−30.290056	150.149194	Mt. Kaputar National Park, New South Wales	No	Yes
W4	−27.300911	152.28361	Esk, Queensland	Yes	Yes

Table A2: Numbers of sires, dams, and phenotyped offspring for each ecotype and population used to estimate genetic variance

Ecotype and population	No. sires	No. dams	No. phenotyped offspring
Dune:			
D1	21	21	114
D3	22	22	122
Total	43	43	236
Headland:			
H1	23	23	151
H2	21	20	121
Total	44	43	272
Tableland:			
T1	20	22	114
T9	17	17	108
Total	37	39	222
Woodland:			
W2	21	23	118
W4	17	15	86
Total	38	38	204

Literature Cited

Abbott, R. J., and H. P. Comes. 2007. Blowin' in the wind: the transition from ecotype to species. New Phytologist 175:197–200.

Ackerly, D. D., S. A. Dudley, S. E. Sultan, J. Schmitt, J. S. Coleman, C. R. Linder, D. R. Sandquist, et al. 2000. The evolution of plant ecophysiological traits: recent advances and future directions. Bioscience 50:979–995.

Agrawal, A. F., E. D. Brodie III, and L. H. Rieseberg. 2001. Possible consequences of genes of major effect: transient changes in the G-matrix. Genetica 112–113:33–43.

Aguirre, J. D., M. W. Blows, and D. J. Marshall. 2014*a*. The genetic covariance between life cycle stages separated by metamorphosis. Proceedings of the Royal Society B 281:20141091.

Aguirre, J. D., E. Hine, K. McGuigan, and M. W. Blows. 2014*b*. Comparing G: multivariate analysis of genetic variation in multiple populations. Heredity 112:21–29.

Alcantara, J. M., J. M. Bastida, and P. J. Rey. 2010. Linking divergent selection on vegetative traits to environmental variation and phenotypic diversification in the Iberian columbines (*Aquilegia*). Journal of Evolutionary Biology 23:1218–1233.

Ali, S. I. 1964. *Senecio lautus* complex in Australia. II. Cultural studies of populations. Australian Journal of Botany 12:292–316.

———. 1969. *Senecio lautus* complex in Australia. V. Taxonomic interpretations. Australian Journal of Botany 17:161–176.

Arnold, S. J. 1992. Constraints on phenotypic evolution. American Naturalist 140(suppl.):S85–S107.

Arnold, S. J., R. Burger, P. A. Hohenlohe, B. C. Ajie, and A. G. Jones. 2008. Understanding the evolution and stability of the G-matrix. Evolution 62:2451–2461.

Arnold, S. J., M. E. Pfrender, and A. G. Jones. 2001. The adaptive landscape as a conceptual bridge between micro- and macroevolution. Genetica 112:9–32.

Barrett, R. D. H., S. M. Rogers, and D. Schluter. 2008. Natural selection on a major armor gene in threespine stickleback. Science 322:255–257.

Barrett, R. D. H., and D. Schluter. 2008. Adaptation from standing genetic variation. Trends in Ecology and Evolution 23:38–44.

Basser, P. J., and S. Pajevic. 2007. Spectral decomposition of a 4th-order covariance tensor: applications to diffusion tensor MRI. Signal Processing 87:220–236.

Bégin, M., and D. A. Roff. 2004. From micro- to macroevolution through quantitative genetic variation: positive evidence from field crickets. Evolution 58:2287–2304.

Blanquart, F., S. Gandon, and S. L. Nuismer. 2012. The effects of migration and drift on local adaptation to a heterogeneous environment. Journal of Evolutionary Biology 25:1351–1363.

Blows, M. W., and K. McGuigan. 2015. The distribution of genetic variance across phenotypic space and the response to selection. Molecular Ecology 24:2056–2072.

Bookstein, F. L., and P. Mitteroecker. 2014. Comparing covariance matrices by relative eigenanalysis, with applications to organismal biology. Evolutionary Biology 41:336–350.

Bylesjo, M., V. Segura, R. Y. Soolanayakanahally, A. M. Rae, J. Trygg, P. Gustafsson, S. Jansson, et al. 2008. LAMINA: a tool for rapid quantification of leaf size and shape parameters. BMC Plant Biology 8:82.

Carriere, Y., and D. A. Roff. 1995. Change in genetic architecture resulting from the evolution of insecticide resistance: a theoretical and empirical analysis. Heredity 75:618–629.

Chenoweth, S. F., H. D. Rundle, and M. W. Blows. 2010. The contribution of selection and genetic constraints to phenotypic divergence. American Naturalist 175:186–196.

Cheverud, J. M. 1982. Phenotypic, genetic, and environmental morphological integration in the cranium. Evolution 36:499–516.

———. 1984. Quantitative genetics and developmental constraints on evolution by selection. Journal of Theoretical Biology 110:155–171.

Colosimo, P. F., K. E. Hosemann, S. Balabhadra, G. Villarreal, M. Dickson, J. Grimwood, J. Schmutz, et al. 2005. Widespread parallel evolution in sticklebacks by repeated fixation of ectodysplasin alleles. Science 307:1928–1933.

Dobzhansky, T. 1956. What is an adaptive trait? American Naturalist 90:337–347.

Doroszuk, A., M. W. Wojewodzic, G. Gort, and J. E. Kammenga. 2008. Rapid divergence of genetic variance-covariance matrix within a natural population. American Naturalist 171:291–304.

Dudley, S. A., and J. Schmitt. 1995. Genetic differentiation in morphological responses to simulated foliage shade between populations of *Impatiens capensis* from open and woodland sites. Functional Ecology 9:655–666.

Eroukhmanoff, F. 2009. Just how much is the G-matrix actually constraining adaptation? Evolutionary Biology 36:323–326.

Eroukhmanoff, F., A. Hargeby, N. N. Arnberg, O. Hellgren, S. Bensch, and E. I. Svensson. 2009. Parallelism and historical contingency during rapid ecotype divergence in an isopod. Journal of Evolutionary Biology 22:1098–1110.

Eroukhmanoff, F., and E. I. Svensson. 2011. Evolution and stability of the G-matrix during the colonization of a novel environment. Journal of Evolutionary Biology 24:1363–1373.

Foster, S. A., G. E. McKinnon, D. A. Steane, B. M. Potts, and R. E. Vaillancourt. 2007. Parallel evolution of dwarf ecotypes in the forest tree *Eucalyptus globulus*. New Phytologist 175:370–380.

Gelman, A. 2006. Prior distributions for variance parameters in hierarchical models. Bayesian Analysis 1:515–533.

Hadfield, J. D. 2010. MCMC methods for multi-response generalized linear mixed models: the MCMCglmm R package. Journal of Statistical Software 33:1–22.

Hansen, T. F., and D. Houle. 2008. Measuring and comparing evolvability and constraint in multivariate characters. Journal of Evolutionary Biology 21:1201–1219.

Hine, E., S. F. Chenoweth, H. D. Rundle, and M. W. Blows. 2009. Characterizing the evolution of genetic variance using genetic covariance tensors. Philosophical Transactions of the Royal Society B 364:1567–1578.

Houle, D., C. Pelabon, G. P. Wagner, and T. F. Hansen. 2011. Measurement and meaning in biology. Quarterly Review of Biology 86:3–34.

Kolbe, J. J., L. J. Revell, B. Szekely, E. D. Brodie III, and J. B. Losos. 2011. Convergent evolution of phenotypic integration and its alignment with morphological diversification in Caribbean *Anolis* ecomorphs. Evolution 65:3608–3624.

Lande, R. 1979. Quantitative genetic analysis of multivariate evolution, applied to brain : body size allometry. Evolution 33:402–416.

———. 1980. The genetic covariance between characters maintained by pleiotropic mutations. Genetics 94:203–215.

Lande, R., and S. J. Arnold. 1983. The measurement of selection on correlated characters. Evolution 37:1210–1226.

Langerhans, R. B. 2010. Predicting evolution with generalized models of divergent selection: a case study with Poeciliid fish. Integrative and Comparative Biology 50:1167–1184.

Langerhans, R. B., and T. J. DeWitt. 2004. Shared and unique features of evolutionary diversification. American Naturalist 164:335–349.

Langerhans, R. B., J. H. Knouft, and J. B. Losos. 2006. Shared and unique features of diversification in greater Antillean *Anolis* ecomorphs. Evolution 60:362–369.

Lewontin, R. C. 1970. The units of selection. Annual Review of Ecology and Systematics 1:1–18.

Losos, J. B. 1990. Ecomorphology, performance capability, and scaling of West Indian *Anolis* lizards: an evolutionary analysis. Ecological Monographs 60:369–388.

Losos, J. B., T. W. Schoener, K. I. Warheit, and D. Creer. 2001. Experimental studies of adaptive differentiation in Bahamian *Anolis* lizards. Genetica 112:399–415.

Lowry, D. B. 2012. Ecotypes and the controversy over stages in the formation of new species. Biological Journal of the Linnean Society 106:241–257.

Lowry, D. B., K. D. Behrman, P. Grabowski, G. P. Morris, J. R. Kiniry, and T. E. Juenger. 2014. Adaptations between ecotypes and along environmental gradients in *Panicum virgatum*. American Naturalist 183:682–692.

Lowry, D. B., J. L. Modliszewski, K. M. Wright, C. A. Wu, and J. H. Willis. 2008*a*. The strength and genetic basis of reproductive isolating barriers in flowering plants. Philosophical Transactions of the Royal Society B 363:3009–3021.

Lowry, D. B., R. C. Rockwood, and J. H. Willis. 2008*b*. Ecological reproductive isolation of coast and inland races of *Mimulus guttatus*. Evolution 62:2196–2214.

Lynch, M., and B. Walsh. 1998. Genetics and analysis of quantitative traits. Sinauer, Sunderland, MA.

Martin, G., E. Chapuis, and J. Goudet. 2008. Multivariate Q_{st}–F_{st} comparisons: a neutrality test for the evolution of the G matrix in structured populations. Genetics 180:2135–2149.

McGuigan, K. 2006. Studying phenotypic evolution using multivariate quantitative genetics. Molecular Ecology 15:883–896.

McGuigan, K., J. D. Aguirre, and M. W. Blows. 2015. Simultaneous estimation of additive and mutational genetic variance in an outbred population of *Drosophila serrata*. Genetics 201:1239–1251.

McGuigan, K., S. F. Chenoweth, and M. W. Blows. 2005. Phenotypic divergence along lines of genetic variance. American Naturalist 165:32–43.

Melo, D., and G. Marroig. 2015. Directional selection can drive the evolution of modularity in complex traits. Proceedings of the National Academy of Sciences of the USA 112:470–475.

Melo, M. C., A. Grealy, B. Brittain, G. M. Walter, and D. Ortiz-Barrientos. 2014. Strong extrinsic reproductive isolation between parapatric populations of an Australian groundsel. New Phytologist 203:323–334.

Melo-Hurtado, M. C. 2014. Ecological speciation in *Senecio lautus*. PhD thesis, University of Queensland.

Muschick, M., A. Indermaur, and W. Salzburger. 2012. Convergent evolution within an adaptive radiation of cichlid fishes. Current Biology 22:2362–2368.

Nosil, P., L. J. Harmon, and O. Seehausen. 2009. Ecological explanations for (incomplete) speciation. Trends in Ecology and Evolution 24:145–156.

Ornduff, R. 1964. Evolutionary pathways of *Senecio lautus* alliance in New Zealand and Australia. Evolution 18:349–360.

Orr, H. A., and A. J. Betancourt. 2001. Haldane's sieve and adaptation from the standing genetic variation. Genetics 157:875–884.

Pritchard, J. K., J. K. Pickrell, and G. Coop. 2010. The genetics of human adaptation: hard sweeps, soft sweeps, and polygenic adaptation. Current Biology 20:R208–R215.

Radford, I. J., R. D. Cousens, and P. W. Michael. 2004. Morphological and genetic variation in the *Senecio pinnatifolius* complex: are variants worthy of taxonomic recognition? Australian Systematic Botany 17:29–48.

Reich, P. B. 2014. The world-wide "fast-slow" plant economics spectrum: a traits manifesto. Ecology 102:275–301.

Richards, T. J., and D. Ortiz-Barrientos. 2016. Immigrant inviability produces a strong barrier to gene flow between parapatric ecotypes of *Senecio lautus*. Evolution 70:1239–1248.

Richards, T. J., G. M. Walter, K. McGuigan, and D. Ortiz-Barrientos. 2016. Divergent natural selection drives the evolution of reproductive isolation in an Australian wildflower. Evolution 70:1993–2003.

Roda, F., L. Ambrose, G. M. Walter, H. L. L. Liu, A. Schaul, A. Lowe, P. B. Pelser, et al. 2013*a*. Genomic evidence for the parallel evolution of coastal forms in the *Senecio lautus* complex. Molecular Ecology 22:2941–2952.

Roda, F., H. L. Liu, M. J. Wilkinson, G. M. Walter, M. E. James, D. M. Bernal, M. C. Melo, et al. 2013*b*. Convergence and divergence during the adaptation to similar environments by an Australian groundsel. Evolution 67:2515–2529.

Roda, F., G. M. Walter, R. Nipper, and D. Ortiz-Barrientos. 2017. Genomic clustering of adaptive loci during parallel evolution of an Australian wildflower. Molecular Ecology 26:3687–3699.

Rosenblum, E. B., and L. J. Harmon. 2011. "Same same but different": replicated ecological speciation at White Sands. Evolution 65:946–960.

Schluter, D. 1995. Adaptive radiation in sticklebacks—trade-offs in feeding performance and growth. Ecology 76:82–90.

———. 1996. Adaptive radiation along genetic lines of least resistance. Evolution 50:1766–1774.

———. 2000. The ecology of adaptive radiation. Oxford University Press, Oxford.

Schluter, D., E. A. Clifford, M. Nemethy, and J. S. McKinnon. 2004. Parallel evolution and inheritance of quantitative traits. American Naturalist 163:809–822.

Turelli, M. 1984. Heritable genetic variation via mutation-selection balance: Lerch's zeta meets the abdominal bristle. Theoretical Population Biology 25:138–193.

Walsh, B., and M. W. Blows. 2009. Abundant genetic variation plus strong selection = multivariate genetic constraints: a geometric view of adaptation. Annual Review of Ecology, Evolution, and Systematics 40:41–59.

Walter, G. M., J. D. Aguirre, M. W. Blows, and D. Ortiz-Barrientos. 2018. Data from: Evolution of genetic variance during adaptive radiation. American Naturalist, Dryad Digital Repository, http://dx.doi.org/10.5061/dryad.m248h.

Walter, G. M., M. J. Wilkinson, M. E. James, T. J. Richards, J. D. Aguirre, and D. Ortiz-Barrientos. 2016. Diversification across a heterogeneous landscape. Evolution 70:1979–1992.

Wood, C. W., and E. D. Brodie III. 2015. Environmental effects on the structure of the G-matrix. Evolution 69:2927–2940.

Zeng, Z. B. 1988. Long-term correlated response, interpopulation covariation, and interspecific allometry. Evolution 42:363–374.

Zhang, X. S., and W. G. Hill. 2005. Genetic variability under mutation selection balance. Trends in Ecology and Evolution 20:468–470.

Associate Editor: Edmund D. Brodie, III
Editor: Alice A. Winn